Journal of Computational Mathematics
Vol.xx, No.x, 2026, 1–34.

http://www.global-sci.org/jcm
doi:10.4208/jcm.2508-m2024-0265

SERENDIPITY VIRTUAL ELEMENT METHOD FOR THE SECOND ORDER ELLIPTIC EIGENVALUE PROBLEM IN TWO AND THREE DIMENSIONS*

Haokun Li, Yulin Liu, Jian Meng and Xu Qian[1)]
College of Science, National University of Defense Technology, Changsha 410073, China
Emails: 18116806158@163.com, 16330677344@163.com, mengjian23@nudt.edu.cn, qianxu@nudt.edu.cn

Abstract

In this paper, we analyze the virtual element method for the symmetric second order elliptic eigenvalue problem with variable coefficients in two and three dimensions, which reduces the number of degrees of freedom of the standard virtual element method. We attempt to prove the interpolation theory and stability analysis for the serendipity nodal virtual element space, which provides new stabilization terms for the virtual element schemes. Then we prove the spectral approximation and the optimal a priori error estimates. Moreover, we construct a fully computable residual-type a posteriori error estimator applied to the adaptive serendipity virtual element method and prove its upper and lower bounds with respect to the approximation error. Finally, we show numerical examples to verify the theoretical results and show the comparison between standard and serendipity virtual element methods.

Mathematics subject classification: 65N25, 65N30, 65N15.
Key words: Serendipity virtual element methods, Self-adjoint elliptic eigenvalue problems, Interpolation estimates, Stability analysis, A priori and a posteriori error estimates.

1. Introduction

In modern scientific and engineering applications, the eigenvalue problems arising from partial differential equations (PDEs) are of fundamental importance in many fields [18, 24, 59, 60]. The numerical approximation of symmetric second order elliptic eigenvalue problem(i.e., reaction-diffusion eigenvalue problem) is a stepping stone towards the more challenging mathematical and engineering problems. There are many numerical methods to solve the eigenvalue problem [3, 25, 40, 66] and finite element method (FEM) is an effective numerical method for the eigenvalue problem [4, 5, 20, 50, 61]. Adaptive FEM is an excellent tool for numerical computation and is even indispensable for certain problems [6]. Until now, the a posteriori error estimates for the symmetric eigenvalue problem have been considered in [2, 28, 32, 33, 36, 41, 44].

The virtual element method (VEM), introduced in [7], is a successful extension of FEM to polygonal/polyhedral meshes. The virtual element space contains a polynomial subspace and the remaining non-polynomial virtual subspace through the introduction of suitable projection operators allowed to be computed by using the degrees of freedom (DoFs) related to the virtual element space. The basis functions are defined by the local PDE problem and never need

* Received November 25, 2024 / Revised version received March 10, 2025 / Accepted August 5, 2025 / Published online January 19, 2026 /
[1)] Corresponding author

the explicit expression. In VEM scheme, a bilinear form contains consistency and stabilization parts, where the consistency on polynomial spaces is assured by the consistency term and the stability of VEM scheme is guaranteed by the other. Meanwhile, VEM is also attractive apart from the mere possibility to use polytopal meshes and is promising in problems related to high-order PDEs and in problems where several useful features are requested at the same time. To date, VEM has been successfully applied to different fields. Regarding to the VEMs for eigenvalue problems, there have been the Steklov eigenvalue problem [52, 54, 55], the Laplacian eigenvalue problem [29, 30, 34, 35, 49], the acoustic vibration problem [17], the vibration and buckling problems of Kirchhoff plate [46, 56, 58], the transmission eigenvalue problem [48, 57], the Stokes eigenvalue problem [43]. Moreover, the great flexibility of VEM becomes appealing in mesh refinement because the locally mesh post-processing to remove hanging nodes is never needed. This naturally motivates us to develop an a posteriori error estimate for the eigenvalue problem. However, the design and analysis of fully computable a posteriori error bounds for VEM is a challenging task. The residual-type a posteriori versions of VEM approximation for the selfadjoint and non-selfadjoint Steklov eigenvalue problems have been investigated in [55,62], respectively. Then a residual-based a posteriori error estimate for the VEM discretization of linear elasticity eigenvalue problem has been also derived in [53]. Recently, the a posteriori error bound for the VEM applied to the Helmholtz transmission eigenvalue problem of anisotropic media has been presented in [47].

However, the standard VEM has more $k-1$ internal DoFs than the classical nodal FEM on a triangular element, where the nonnegative integer number k denotes the degree of the approximate polynomial space. It is meaningful that a new variant of nodal VEM that mimics serendipity FEM is introduced in [11]. Serendipity virtual element method (SVEM) allows for a reduction of the number of internal DoFs without affecting the convergence and stability properties of VEMs. To cope with a sufficiently wide range of problems in mixed forms and electromagnetic problems [21, 51], the extensions of face and edge virtual elements were developed in [8, 9, 13, 14]. The interpolation theory and stability analysis associated to serendipity nodal, face and edge virtual element spaces are proved in [15, 16]. Very recently, the performance of serendipity VEMs in solving semilinear parabolic integro-differential equations [64] and the semilinear pseudo-parabolic equations on curved domains [65] are investigated. However, the work about the 3D serendipity VEM is very limited, which is also the topic of the present work.

In this paper, we first rigorously prove the interpolation theory of the nodal SVEM inspired by the existing theoretical results in [16]. Besides, we give the stability analysis for the defined stabilization. Then the correct spectral approximation and the optimal a priori error estimates of the SVEM scheme are established. In addition, we construct a fully computable residual-type a posteriori error estimator, which contains the element and edge residuals and the terms related to the inconsistency of the virtual element scheme. For the eigenvalue problem with variable coefficients, there are some element and edge data oscillation terms in the lower bound, however, we only need to mark the desired refined elements according to the well-defined error estimator that does not contain these oscillation terms in practice. We prove that the estimator is both reliable and efficient with respect to the approximation error. Numerical results are shown to support our theoretical analysis.

The remainder of this paper is structured as follows. In Section 2, we introduce the model problem and the continuous solution operator. In Section 3, we present the SVEM, including the definition of serendipity nodal virtual elements, interpolation error estimates and the stabilized serendipity virtual element scheme. In Section 4, we prove the a priori error estimates and

a posteriori error estimates of the SVEM scheme. In Section 5, we report a series of numerical tests to verify our theoretical results. Finally, conclusions are drawn in Section 6.

2. The Self-adjoint Elliptic Eigenvalue Problem

Throughout the paper, we will use the standard notation for Sobolev space $W^{s,p}(D)$ equipped with the norm $\|\cdot\|_{s,p,D}$ and seminorm $|\cdot|_{s,p,D}$ on a bounded domain $D \subseteq \mathbb{R}^d$ $(d = 1, 2, 3)$, where we denote sets of coordinates in two dimensions by $\boldsymbol{x} = (x_1, x_2)^\top \in \mathbb{R}^2$ and in three dimensions by $\boldsymbol{x} = (x_1, x_2, x_3)^\top \in \mathbb{R}^3$. We also denote the diameter by h_D and the measure by $|D|$ for a geometric object D, respectively. For $p = 2$, we denote $H^s(D) = W^{s,2}(D)$, and the subscript p in the associated norm and seminorm will be omitted. The space $H^0(D)$ coincides with the Lebesgue space $L^2(D)$, and the inner product on $L^2(D)$ is denoted by $(\cdot, \cdot)_D$. The subscript D will be omitted when D denotes the whole computational domain. For a nonnegative integer $k, \mathbb{P}_k(D)$ denotes the space of polynomials on D of degree at most k. Meanwhile, the set of scaled monomials with the degree k on the domain D is defined by

$$M_k(D) = \left\{ \left(\frac{\boldsymbol{x} - \boldsymbol{b}_D}{h_D} \right)^{\boldsymbol{s}}, \ |\boldsymbol{s}| \le k \right\},$$

where $\boldsymbol{b}_D$ is the barycenter of D and $\boldsymbol{s} = (s_1, s_2, \cdots, s_d)$ is a multi-index with

$$|\boldsymbol{s}| = s_1 + s_2 + \cdots + s_d.$$

As usual, we use bold fonts to express vector and matrix variables, operators, spaces.

Assume $\Omega \subseteq \mathbb{R}^d$ $(d = 2, 3)$ is a bounded simply connected domain with boundary $\partial\Omega$. Let $u(\boldsymbol{x})$ be a scalar function and ∇u be its gradient representation given by $\nabla u = (\partial_{x_1} u, \partial_{x_2} u)^\top$ in $\mathbb{R}^2$ and $\nabla u = (\partial_{x_1} u, \partial_{x_2} u, \partial_{x_3} u)^\top$ in $\mathbb{R}^3$. The symmetric elliptic eigenvalue problem is stated as: Find non-zero u such that $\|u\|_0 = 1$ and

$$\begin{aligned} -\mathrm{div}(\mathbf{A}\nabla u) + \rho u &= \lambda u \quad \text{in } \Omega, \\ u &= 0 \qquad\qquad\ \text{on } \partial\Omega, \end{aligned} \tag{2.1}$$

where $\mathbf{A}$ is a uniformly bounded and symmetric positive definite matrix with sufficiently smooth real entries and ρ is a uniformly bounded and sufficiently smooth nonnegative real scalar function. Multiplying (2.1) by test function $v \in H_0^1(\Omega)$, it follows from integrating by parts that the variational form of (2.1) can be written as: Find non-zero $(\lambda, u) \in \mathbb{R} \times H_0^1(\Omega)$ such that

$$\mathbb{A}(u, v) = \lambda b(u, v), \quad \forall\, v \in H_0^1(\Omega), \tag{2.2}$$

where the bilinear forms are defined by

$$a^{\mathbf{A}}(u, v) := (\mathbf{A}\nabla u, \nabla v), \quad b(\rho u, v) := (\rho u, v), \quad \mathbb{A}(u, v) = a^{\mathbf{A}}(u, v) + b(\rho u, v).$$

To study the spectral approximation for the problem (2.2), we introduce the continuous solution operator

$$T : H_0^1(\Omega) \ \to \ H_0^1(\Omega), \quad Tf = \mu, \tag{2.3}$$

where μ is the solution of the following corresponding source problem: For any given $f \in H_0^1(\Omega)$, find $\mu \in H_0^1(\Omega)$ such that

$$\mathbb{A}(\mu, v) = b(f, v), \quad \forall\, v \in H_0^1(\Omega). \tag{2.4}$$

Since the problem (2.2) does not admit the null eigenvalue, then λ is an eigenvalue of (2.2) if and only if $1/\lambda$ is an eigenvalue of T associated to the same eigenvector $T(\lambda u)$.

Then we discuss the properties of the continuous solution operator T, whose spectrum is related with the solutions of the eigenvalue problem. To show the existence of T, we need to check the well-posedness of (2.4). It is clear that $\mathbb{A}(\cdot,\cdot)$ is coercive and bounded over $H_0^1(\Omega)$. By the Lax-Milgram theorem, there exists a unique solution $\mu \in H_0^1(\Omega)$ to the problem (2.4). Then the solution operator T is well-defined by the Riesz representation theorem.

In the error analysis, the regularity of the solution μ to the source problem is necessary. According to the regularity results in [37,39], the following regularity assumption for the source problem (2.4) holds in this paper: there exists a constant $r_\Omega > 0$ such that $\mu \in H^{1+r}(\Omega)$ with for any $r \in (0, r_\Omega)$ for each $f \in L^2(\Omega)$, furthermore,

$$\|\mu\|_{1+r} \leq C\|f\|_0, \tag{2.5}$$

where $r_\Omega \geq 1$ if Ω is a convex domain, while it is at least $\pi/\omega - \varepsilon$ (for any $\varepsilon > 0$) for the non-convex domain with maximum interior angle $\omega < 2\pi$.

Due to compact inclusion $H^{1+r}(\Omega) \hookrightarrow H_0^1(\Omega)$, the solution operator T is compact. From the spectral theory of compact operator, we can conclude the result of the spectral characterization as follows: The spectrum set $\mathrm{sp}(T)$ has 0 as the only accumulation point and the multiplicity of each non-zero eigenvalue is finite. For more discussions of the corresponding spectral theory, see also [5, 45].

3. Serendipity Virtual Element Method

3.1. Mesh assumptions

Let $\mathcal{T}_h$ be a partition of Ω into non-overlapping polytopal elements, $\mathcal{B}_h^f$ be the set of all two-dimensional faces, and $\mathcal{B}_h^e$ be the set of all one-dimensional edges. The following mesh regularity assumptions are satisfied [1, 7, 11]:

$d = 2$. There exists a uniform constant $C > 0$ independent of mesh size h such that

(i) every polygonal element E is star-shaped with respect to a disk of radius $\geq Ch_E$;

(ii) every edge $e \in \partial E$ satisfies $h_e \geq Ch_E$.

$d = 3$. There exists a uniform constant $C > 0$ independent of mesh size h such that

(i) every polyhedral element E is star-shaped with respect to a ball of radius $\geq Ch_E$;

(ii) every face $F \in \partial E$ is star-shaped with respect to a disk of radius $\geq Ch_F$;

(iii) every edge $e \in \partial F$ satisfies $h_e \geq Ch_F \geq C^2 h_E$.

Remark 3.1. An immediate consequence of the above mesh regularity assumptions is that each element E admits a shape-regular partition into simplices $\mathcal{T}_E$ [26]. In the following, the adaptive VEM mesh decompositions and some extended techniques on polytopal elements hinge upon the existence of the shape-regular simplicial tessellation.

Remark 3.2. For the sake of simplicity, we restrict the following convexity assumption: (iv) every polygonal element/general face is convex and there exists a constant $\varepsilon > 0$ such that each internal angle θ of element E satisfies $\varepsilon \leq \theta \leq \pi - \varepsilon$. The nonconvex case would result in more complex definitions, but may be tackled along the same lines as the convex case. We refer the reader to [10, 11, 13] for the necessary background.

3.2. Standard and serendipity virtual element spaces

We start with the following finite-dimensional space on the 2D polygonal element E, which can be also regarded as a generic face of the 3D polyhedron element

$$V_h^k(E) = \big\{v \in H^1(E) : v|_e \in \mathbb{P}_k(e),\ \forall\, e \in \partial E,\ \Delta v \in \mathbb{P}_k(E)\big\}. \tag{3.1}$$

For each function v_h in $V_h^k(E)$, the unisolvent scaled DoFs are endowed with [8, Proposition 3.1]

D_1^{2D}: the values of v_h at all vertices of E;

D_2^{2D}: the values of v_h at the $(k-1)$ internal Gauss-Lobatto nodes on each edge e of E;

D_3^{2D}: the internal moments of v_h on element E up to order k: $|E|^{-1}(v_h, m_k)_E,\ \forall\, m_k \in M_k(E)$.

We denote the i-th local DoF by χ_i with $i = 1, \ldots, N_D$. It is also readily checked that $\mathbb{P}_k(E) \subseteq V_h^k(E)$, which guarantees the optimal accuracy of the VEM approximation. By [31, Theorem 3.6], we observe the validity of the following inverse estimate on the virtual element space $V_h^k(E)$:

$$\|\nabla v_h\|_{0,E} \le C h_E^{-1} \|v_h\|_{0,E}, \quad \forall\, v_h \in V_h^k(E). \tag{3.2}$$

From mesh regularity assumptions in Section 3.1, the following polynomial projection error holds true.

Proposition 3.1 ([23, 54]). *For each $v \in H^{1+r}(E)$ with $0 < r \le k$, there exists $v_\pi \in \mathbb{P}_k(E)$ such that*

$$\|v - v_\pi\|_{0,E} + h_E |v - v_\pi|_{1,E} \le C h_E^{1+r} \|v\|_{1+r,E}. \tag{3.3}$$

For each $v \in H^{1+r}(E)$ with $r > 0$, the interpolation operator $\tilde{I}_h^E$ on the space $V_h^k(E)$ is defined by DoFs D_1^{2D}-D_2^{2D}-D_3^{2D} as follows:

$$\chi_i\big(\tilde{I}_h^E v\big) = \chi_i(v), \quad i = 1, \ldots, N_D. \tag{3.4}$$

We can obtain the interpolation estimates in [22, 26, 31, 38, 42].

Proposition 3.2. *For each $v \in H^{1+r}(E)$ with $0 < r \le k$, we have*

$$\big\|v - \tilde{I}_h^E v\big\|_{0,E} + h_E \big|v - \tilde{I}_h^E v\big|_{1,E} \le C h_E^{1+r} \|v\|_{1+r,E}. \tag{3.5}$$

3.3. 2D serendipity virtual element space and interpolation estimates

As in [8,9,11,13], we set η_E as the minimum number of straight lines necessary to cover the boundary of E and define $\beta_E = k - \eta_E$. Notably, η_E must not be smaller than 3. In order to define the serendipity space, we define a projection $\Pi_{k,E}^s : V_h^k(E) \to \mathbb{P}_k(E)$ by

$$\beta_E < 0 : \int_{\partial E} \big(v_h - \Pi_{k,E}^s v_h\big) p_k \mathrm{d}s = 0, \qquad \forall\, p_k \in \mathbb{P}_k(E), \tag{3.6a}$$

$$\beta_E \ge 0 : \begin{cases} \displaystyle\int_{\partial E} \big(v_h - \Pi_{k,E}^s v_h\big) p_{\eta_E} \mathrm{d}s = 0, & \forall\, p_{\eta_E} \in \mathbb{P}_{\eta_E}(E), \\ \displaystyle\int_{E} \big(v_h - \Pi_{k,E}^s v_h\big) p_{\beta_E} \mathrm{d}E = 0, & \forall\, p_{\beta_E} \in \mathbb{P}_{\beta_E}(E). \end{cases} \tag{3.6b}$$

For the completeness, we discuss the well-posedness of the introduced projection $\Pi_{k,E}^s$.

Proposition 3.3. *The projection operator $\Pi^s_{k,E}$ is well defined.*

Proof. It can be checked that the number of conditions for the projector $\Pi^s_{k,E}$ is equal to the dimension of $\mathbb{P}_k(E)$. Then it suffices to check that the conditions

$$\beta_E < 0 : \int_{\partial E} \Pi^s_{k,E} v_h p_k \mathrm{d}s = 0, \qquad \forall\, p_k \in \mathbb{P}_k(E), \tag{3.7a}$$

$$\beta_E \geq 0 : \begin{cases} \displaystyle\int_{\partial E} \Pi^s_{k,E} v_h p_{\eta_E} \mathrm{d}s = 0, & \forall\, p_{\eta_E} \in \mathbb{P}_{\eta_E}(E), \\ \displaystyle\int_{E} \Pi^s_{k,E} v_h p_{\beta_E} \mathrm{d}E = 0, & \forall\, p_{\beta_E} \in \mathbb{P}_{\beta_E}(E) \end{cases} \tag{3.7b}$$

imply $\Pi^s_{k,E} v_h \equiv 0$. By (3.7a), we have $(\Pi^s_{k,E} v_h)|_{\partial E} = 0$. Therefore, if $\beta_E < 0$, the above result is sufficient to give $\Pi^s_{k,E} v_h \equiv 0$ by [23, Lemma 3.1.10].

On the other hand, if $\beta_E \geq 0$, by $(\Pi^s_{k,E} v_h)|_{\partial E} = 0$ and using [23, Lemma 3.1.10] again, it follows that there exists $p^*_{\beta_E} \in \mathbb{P}_{\beta_E}(E)$ such that

$$\Pi^s_{k,E} v_h = b_{\eta_E} p^*_{\beta_E}, \tag{3.8}$$

where $b_{\eta_E} > 0$ is the polynomial of degree η_E that vanishes identically on ∂E and is equal to 1 at the barycenter of the element E; see [11, Section 3]. Then we substitute (3.8) into (3.7b) and take $p_{\beta_E} = p^*_{\beta_E}$ in (3.7b) to obtain

$$\int_E b_{\eta_E} \big(p^*_{\beta_E}\big)^2 \mathrm{d}E = 0, \tag{3.9}$$

which concludes $p^*_{\beta_E} \equiv 0$ and thus $\Pi^s_{k,E} v_h \equiv 0$ by (3.8). □

Remark 3.3. To handle the serendipity VEM, we have assumed the additional convexity condition (iv) in Section 3.1. From the proof, such a condition can be relaxed for the particular case $\beta_E < 0$.

Remark 3.4. In practice, the computation of such a η_E on each element E could be a heavy task. We here provide a hint that η_E is equal to the number of edges for strictly convex polygons. In this case, η_E always ≥ 3, a lazy choice could be to take $\eta_E = 3$ for all the elements; while a stingy choice would compute the exact η_E for each element. Besides, the condition defining η_E is inherently unstable due to the presentence of very small edges or edges laying almost on the same line. Inspired by [11], the strategy adopted in code states follows: we can fix an angle threshold θ and an edge ratio ρ. If two edges form an angle bigger than θ, these two edges will be regards as a single edge; the edges having length smaller than ρh_E are neglected; see [11] for more details.

Remark 3.5. There exist many choices of the projection operator $\Pi^s_{k,E}$. In principle, a proper choice could allow a strategy towards the defined serendipity virtual element space with suitable properties.

Based on the space $V^k_h(E)$ and the projection operator $\Pi^s_{k,E}$, we define the serendipity virtual element space on the local element E as

$$SV^k_h(E) = \left\{ v_h \in V^k_h(E) : \int_E \big(v_h - \Pi^s_{k,E} v_h\big) p \,\mathrm{d}E = 0,\ \forall\, p \in \mathbb{P}_{k/\beta_E}(E) \right\}, \tag{3.10}$$

where $\mathbb{P}_{k/\beta_E}(E)$ denotes the space spanned by the homogeneous polynomials of degree r with $\beta_E < r \leq k$. It could be checked that $\mathbb{P}_k(E) \subseteq SV_h^k(E) \subseteq V_h^k(E)$. A set of unisolvent DoFs $\{\chi_i^s\}_{i=1}^{N_{SD}}$ of the space $SV_h^k(E)$ is given by D_1^{2D}, D_2^{2D}, the moments of order up to k can be computed by those of the projection $\Pi_{k,E}^s$; see (3.10).

Remark 3.6. Recalling the definition of the standard virtual element space in [1] as follows:

$$W_h^k(E) = \left\{ v_h \in V_h^k(E) : \int_E \big(v_h - \Pi_{k,E}^\nabla v_h\big) p \,\mathrm{d}E = 0,\ \forall\, p \in \mathbb{P}_{k/k-2}(E) \right\}, \tag{3.11}$$

which has been applied to the eigenvalue problem in [35]. Here, the projection operator $\Pi_{k,E}^\nabla : H^1(E) \to \mathbb{P}_k(E)$ is defined by

$$\int_E \nabla\big(\Pi_{k,E}^\nabla v - v\big) \cdot \nabla p_k \mathrm{d}E = 0, \quad P_0\big(\Pi_{k,E}^\nabla v - v\big) = 0, \quad \forall\, v \in H^1(E), \quad \forall\, p_k \in \mathbb{P}_k(E), \tag{3.12}$$

where we choose

$$P_0(v) = \frac{1}{N_E^V} \sum_{i=1}^{N_E^V} v(V_i), \quad k = 1,$$
$$P_0(v) = \frac{1}{|E|} \int_E v \,\mathrm{d}E, \qquad k \geq 2.$$

Since β_E is not bigger than $k-3$, then our choice reduces by $(\pi_{k-2,2} - \pi_{\beta_E,2})$ internal DoFs of the standard virtual element space $W_h^k(E)$, where $\pi_{k,2}$ denotes the dimension of the polynomial space $\mathbb{P}_k(E)$.

Remark 3.7. If $\beta_E < 0$, the serendipity virtual element space is only endowed with the boundary DoFs.

Inspired by [8, Lemma 5.3], we have

$$\nabla \Pi_{k,E}^s v = \Pi_{S,E}^e \nabla v, \quad \forall\, v \in H^1(E), \tag{3.13}$$

where $\Pi_{S,E}^e$ is the required projection when defining the serendipity edge virtual element space and its error estimate has been proven in [16, Theorem 3.2] as follows:

$$\big\|v - \Pi_{S,E}^e v\big\|_{0,E} \leq C h_E^{1+r} |v|_{1+r,E}, \quad \forall\, v \in \big(H^{1+r}(E)\big)^2, \quad 0 < r \leq k. \tag{3.14}$$

The following lemma contains a useful estimate for the polynomial projection $\Pi_{k,E}^s$.

Lemma 3.1. *For each $v \in H^{1+r}(E)$ with $0 < r \leq k$, we have*

$$\big\|\nabla\big(v - \Pi_{k,E}^s v\big)\big\|_{0,E} \leq C h_E^r |v|_{1+r,E}. \tag{3.15}$$

Proof. By (3.13) and (3.14), it follows that

$$\big\|\nabla\big(v - \Pi_{k,E}^s v\big)\big\|_{0,E} = \big\|\nabla v - \Pi_S^e \nabla v\big\|_{0,E} \leq C h_E^r |v|_{1+r,E}. \tag{3.16}$$

Thus, we complete the proof. □

The interpolation operator I_h^E on the space $SV_h^k(E)$ is well defined for each function v in $H^{1+r}(E)$ with $r > 0$, by such DoFs, i.e.,

$$\chi_i^s\big(I_h^E v\big) = \chi_i^s(v), \quad i = 1, 2, \ldots, N_{SD}. \tag{3.17}$$

Next, we prove the interpolation estimates for I_h^E on the serendipity virtual element space $SV_h^k(E)$.

Theorem 3.1. *For each $v \in H^{1+r}(E)$ with $0 < r \leq k$, we have*

$$\left\|v - I_h^E v\right\|_{0,E} + h_E \left|v - I_h^E v\right|_{1,E} \leq C h_E^{1+r} \|v\|_{1+r,E}. \tag{3.18}$$

Proof. Recalling that $\tilde{I}_h^E v$ is the interpolation of v on $V_h^k(E)$ and using the H^1-orthogonal decomposition in [31, Lemma 3.3], we can define a function $\psi \in H^1(E)$ satisfying

$$\Delta\psi = 0 \quad \text{in } E, \quad \psi = \tilde{I}_h^E v - I_h^E v \quad \text{on } \partial E, \tag{3.19}$$

and the other function $\phi \in H^1(E)$ satisfying

$$\Delta\phi = \Delta\big(\tilde{I}_h^E v - I_h^E v\big) \quad \text{in } E, \quad \phi = 0 \quad \text{on } \partial E \tag{3.20}$$

such that

$$\tilde{I}_h^E v - I_h^E v = \psi + \phi, \quad \left\|\nabla\big(\tilde{I}_h^E v - I_h^E v\big)\right\|_{0,E}^2 = \|\nabla\psi\|_{0,E}^2 + \|\nabla\phi\|_{0,E}^2. \tag{3.21}$$

From the definitions (3.4) and (3.17) of $\tilde{I}_h^E v$ and $I_h^E v$, using also (3.19), we deduce

$$\tilde{I}_h^E v - I_h^E v = 0 \quad \text{on } \partial E \implies \psi = 0 \quad \text{in } E. \tag{3.22}$$

Furthermore, we have $\Pi_{k,E}^s(I_h^E v) = \Pi_{k,E}^s v$ since $I_h^E v$ and v share the same DoFs and the value of the projection $\Pi_{k,E}^s$ only depends on such DoFs. By integrating by parts, (3.20), (3.22), (3.21), the fact that $\Delta(\tilde{I}_h v - I_h v) \in \mathbb{P}_k$, (3.6a), (3.10) and Lemma 3.1, we write

$$\begin{aligned}
\|\nabla\phi\|_{0,E}^2 &= -(\Delta\phi, \phi)_E = -\big(\Delta\big(\tilde{I}_h^E v - I_h^E v\big), \tilde{I}_h^E v - I_h^E v\big)_E \\
&= -\big(\Delta\big(\tilde{I}_h^E v - I_h^E v\big), v - \Pi_{k,E}^s\big(I_h^E v\big)\big)_E \\
&= -\big(\Delta\big(\tilde{I}_h^E v - I_h^E v\big), v - \Pi_{k,E}^s v\big)_E \\
&= \big(\nabla\big(\tilde{I}_h^E v - I_h^E v\big), \nabla\big(v - \Pi_{k,E}^s v\big)\big)_E \\
&\leq \left\|\nabla\big(\tilde{I}_h^E v - I_h^E v\big)\right\|_{0,E} \left\|\nabla\big(v - \Pi_{k,E}^s v\big)\right\|_{0,E} \\
&\leq C h_E^r |v|_{1+r,E} \left\|\nabla\big(\tilde{I}_h^E v - I_h^E v\big)\right\|_{0,E}.
\end{aligned} \tag{3.23}$$

Combining (3.22), (3.23) and (3.21), we obtain

$$\left\|\nabla\big(\tilde{I}_h^E v - I_h^E v\big)\right\|_{0,E} \leq C h_E^r |v|_{1+r,E}. \tag{3.24}$$

On the other hand, by the fact $\tilde{I}_h^E v - I_h^E v = 0$ on ∂E and then using the Poincaré-Friedrichs inequality and (3.24), we derive

$$\left\|\tilde{I}_h^E v - I_h^E v\right\|_{0,E} \leq C h_E \left\|\nabla\big(\tilde{I}_h^E v - I_h^E v\big)\right\|_{0,E} \leq C h_E^{1+r} |v|_{1+r,E}. \tag{3.25}$$

Therefore, the bound (3.18) follows by the triangle inequality and the obtained error estimates (3.24), (3.25) for $\tilde{I}_h^E v - I_h^E v$. □

3.4. 3D serendipity virtual element space

The construction of the virtual element space in 3D case is recursive. Noticing that for every polyhedral element E in 3D, any face $F \in \partial E$ is now a polygon. We begin with defining the virtual elements on each face $F \in \partial E$. We introduce the boundary space

$$\mathcal{B}^k(\partial E) = \left\{v_h \in C^0(\partial E) : v_h|_F \in SV_h^k(F),\ \forall\, F \in \partial E\right\}, \tag{3.26}$$

where these functions are 2D virtual element functions on each face and are continuous across the edges. Then the virtual element space on the polyhedron E is defined by

$$SV_h^k(E) = \Big\{ v_h \in H^1(E) :\ v_h|_{\partial E} \in \mathcal{B}^k(\partial E),\ \Delta v_h \in \mathbb{P}_k(E), \\ \int_E (v_h - \Pi^{\nabla}_{k,E} v_h) p \,\mathrm{d}E = 0,\ \forall\, p \in \mathbb{P}_{k/(k-2)}(E) \Big\},$$

where the projection operator $\Pi^{\nabla}_{k,E}$ is the 3D counterpart of (3.12). Moreover, we apply the same mathematical symbols as the two-dimensional case for brevity. In the spirit of the 2D case, the degrees of freedom of the three-dimensional VEM space can be taken as

SD_1^{3D}: the values of v_h at all vertices of E;

SD_2^{3D}: the values of v_h at the $(k-1)$ internal Gauss-Lobatto nodes on each edge $e \in \partial F$;

SD_3^{3D}: the moments of v_h on element E up to order $k-2$: $|E|^{-1}(v_h, m_{k-2})_E,\ \forall\, m_{k-2} \in M_{k-2}(E)$.

In conclusion, we introduce the three-dimensional serendipity VEM space by changing two-dimensional boundary VEM space into serendipity version. Moreover, the corresponding theoretical analysis of the interpolation estimates in 3D is also an extended version of the two-dimensional companion. Eventually, by gluing the local space $SV_h^k(E)$ over all elements $E \in \mathcal{T}_h$, we can construct the global serendipity virtual element space

$$SV_h^k := \big\{ v_h \in H_0^1(\Omega) : v_h|_E \in SV_h^k(E),\ \forall\, E \in \mathcal{T}_h \big\}. \tag{3.27}$$

Any global operator can be also locally defined, for instance, $\Pi_k^0|_E := \Pi^0_{k,E}$ and $I_h|_E := I_h^E$.

3.5. Serendipity virtual element scheme and stability analysis

In this section, we are devoted to the SVEM scheme for the eigenvalue problem (2.2). First of all, we discuss the computability of the required projection operators:

2D $\Pi^s_{k,E}$: For each $v_h \in SV_h^k(E)$,

$$\int_{\partial E} \Pi^s_{k,E} v_h p_k \mathrm{d}s = \int_{\partial E} v_h p_k \mathrm{d}s, \\ \int_E \Pi^s_{k,E} v_h p_{\beta_E} \mathrm{d}E = \int_E v_h p_{\beta_E} \mathrm{d}E,$$

where all the terms on the right-hand side are computable since $v_h|_{\partial E}$ is a k-degree polynomial and $\int_E v_h p_{\beta_E} \mathrm{d}E$ can be computed by the degrees of freedom SD_3^{2D}.

2D $\Pi^{\nabla}_{k,E}$:

$$\int_E \nabla \Pi^{\nabla}_{k,E} v_h \cdot \nabla p_k \mathrm{d}E = \int_E \nabla v_h \cdot \nabla p_k \mathrm{d}E \\ = \int_{\partial E} v_h \frac{\partial p_k}{\partial \boldsymbol{n}_{\partial E}} \mathrm{d}s - \int_E v_h \Delta p_k \mathrm{d}E,$$

where the right-hand terms are computable from the degrees of freedom and the projection $\Pi^s_{k,E}$, see (3.10).

2D $\Pi^0_{k,E}$: The L^2-projection operator $\Pi^0_{k,E} : SV^k_h(E) \to \mathbb{P}_k(E)$ can be also computed by these DoFs and using the projection $\Pi^s_{k,E}$.

2D $\mathbf{\Pi}^0_{k-1,E}$: The L^2-projection $\mathbf{\Pi}^0_{k-1,E}$ of the vector function ∇v_h onto $(\mathbb{P}_{k-1}(E))^2$ is computable. Indeed, we have

$$\begin{aligned}&\int_E \mathbf{\Pi}^0_{k-1,E}\nabla v_h \cdot \boldsymbol{p}_{k-1}\mathrm{d}E = \int_E \nabla v_h \cdot \boldsymbol{p}_{k-1}\mathrm{d}E\\ =&\int_{\partial E} v_h \boldsymbol{p}_{k-1}\cdot \boldsymbol{n}_{\partial E}\mathrm{d}s - \int_E v_h \mathrm{div}\,\boldsymbol{p}_{k-1}\mathrm{d}E\\ =&\int_{\partial E} v_h \boldsymbol{p}_{k-1}\cdot \boldsymbol{n}_{\partial E}\mathrm{d}s - \int_E \mathbf{\Pi}^0_{k-1,E} v_h \mathrm{div}\,\boldsymbol{p}_{k-1}\mathrm{d}E.\end{aligned}$$

3D $\Pi^\nabla_{k,E}$: By lending the two-dimensional projection $\Pi^0_{k,F}$ on the face $F \in \partial E$, we derive

$$\begin{aligned}&\int_E \nabla\Pi^\nabla_{k,E} v_h \cdot \nabla p_k\mathrm{d}E = \int_E \nabla v_h \cdot \nabla p_k\mathrm{d}E\\ =&\int_{\partial E} v_h \frac{\partial p_k}{\partial \boldsymbol{n}_{\partial E}}\mathrm{d}F - \int_E v_h \Delta p_k\mathrm{d}E\\ =&\sum_{F\in\partial E}\int_F \Pi^0_{k,F} v_h \frac{\partial p_k}{\partial \boldsymbol{n}_F}\mathrm{d}F - \int_E v_h\Delta p_k\mathrm{d}E.\end{aligned}$$

3D $\Pi^0_{k,E}$: The standard L^2-projection operator $\Pi^0_{k,E} : SV^k_h(E) \to \mathbb{P}_k(E)$ is computable from

$$\int_E \Pi^0_{k,E} v_h \cdot p_k\mathrm{d}E = \begin{cases}\displaystyle\int_E \Pi^\nabla_{k,E} v_h \cdot p\mathrm{d}E, & \forall\, p \in \frac{\mathbb{P}_k(E)}{\mathbb{P}_{k-2}(E)},\\ \displaystyle\int_E v_h \cdot p\mathrm{d}E, & \forall\, p \in \mathbb{P}_{k-2}(E).\end{cases}$$

3D $\mathbf{\Pi}^0_{k-1,E}$:

$$\begin{aligned}&\int_E \mathbf{\Pi}^0_{k-1,E}\nabla v_h \cdot \boldsymbol{p}_{k-1}\mathrm{d}E = \int_E \nabla v_h \cdot \boldsymbol{p}_{k-1}\mathrm{d}E\\ =&\int_{\partial E} v_h \boldsymbol{p}_{k-1}\cdot \boldsymbol{n}_{\partial E}\mathrm{d}F - \int_E v_h \mathrm{div}\,\boldsymbol{p}_{k-1}\mathrm{d}E\\ =&\sum_{F\in\partial E}\int_F \big(\Pi^0_{k,F} v_h\big)\boldsymbol{p}_{k-1}\cdot \boldsymbol{n}_F\mathrm{d}F - \int_E v_h \mathrm{div}\,\boldsymbol{p}_{k-1}\mathrm{d}E.\end{aligned}$$

Moreover, the following estimate was established in [12]:

$$\big|v_h - \Pi^\nabla_{k,E} v_h\big|_{1,E} \le \big|v_h - \Pi^0_{k,E} v_h\big|_{1,E}. \tag{3.28}$$

Let $S^E_a(\cdot\,,\cdot)$ and $S^E_b(\cdot\,,\cdot)$ be symmetric, positive definite and computable bilinear forms, which shall be fixed in the following. For $u_h, v_h \in SV^k_h(E)$, we define the following discrete bilinear forms on the element level:

$$a^{\mathbf{A},E}_h(u_h, v_h) = b^E\big(\mathbf{A}\mathbf{\Pi}^0_{k-1,E}\nabla u_h, \mathbf{\Pi}^0_{k-1,E}\nabla v_h\big) + S^E_a\big(\big(I - \Pi^\nabla_{k,E}\big)u_h, \big(I - \Pi^\nabla_{k,E}\big)v_h\big), \tag{3.29}$$

$$b^E_h(\rho u_h, v_h) = b^E\big(\rho\Pi^0_{k,E} u_h, \Pi^0_{k,E} v_h\big) + S^E_b\big(\big(I - \Pi^0_{k,E}\big)u_h, \big(I - \Pi^0_{k,E}\big)v_h\big). \tag{3.30}$$

Remark 3.8. In view of the detailed discussion in [12] for the VEM bilinear form associated to the diffusion term with variable coefficients, we apply the VEM discretization (3.29), instead of

$$a_h^{\mathbf{A},E}(u_h,v_h)=b^E\big(\mathbf{A}\nabla\Pi_{k,E}^{\nabla}u_h,\nabla\Pi_{k,E}^{\nabla}v_h\big)+S_a^E\big(\big(I-\Pi_{k,E}^{\nabla}\big)u_h,\big(I-\Pi_{k,E}^{\nabla}\big)v_h\big),\tag{3.31}$$

which will show heavy loss of convergence.

Thanks to the definitions of the bilinear forms $a_h^{\mathbf{A},E}(\cdot\,,\cdot)$ and $b_h^E(\cdot\,,\cdot)$, we have the essential property of polynomial consistency on the serendipity virtual element space, see, e.g., [12,26,27].

Proposition 3.4. *The bilinear forms $a_h^{\mathbf{I},E}(\cdot\,,\cdot)$ and $b_h^E(\cdot\,,\cdot)$ satisfy the following k-consistency: For each $v_h\in SV_h^k(E)$ and $p_k\in\mathbb{P}_k(E)$, we have*

$$a_h^{\mathbf{I},E}(v_h,p_k)=b^E(\nabla v_h,\nabla p_k),\quad b_h^E(v_h,p_k)=b^E(v_h,p_k).\tag{3.32}$$

Next, we define computable stabilizations for the serendipity VEM discretization and prove the stability property. Before proving the stability property, we first introduce the following lemma in [31, Theorem 4.5].

Lemma 3.2. *Let $\boldsymbol{\chi}(v_h)$ be a vector denoted by $\boldsymbol{\chi}(v_h):=(\chi_1(v_h),\cdots\chi_{N_D}(v_h))$ for each $v_h\in V_h^k(E)$. Then the following norm equivalence is valid:*

$$C_1h_E\|\boldsymbol{\chi}(v_h)\|_{l^2}\le\|v_h\|_{0,E}\le C_2h_E\|\boldsymbol{\chi}(v_h)\|_{l^2},\tag{3.33}$$

where the norm $\|\cdot\|_{l^2}$ denotes the usual discrete l^2-norm.

Corollary 3.1. *Let $\boldsymbol{\chi}^s(v_h)$ be a vector denoted by $\boldsymbol{\chi}^s(v_h):=(\chi_1^s(v_h),\cdots\chi_{N_{SD}}^s(v_h))$ for each $v_h\in SV_h^k(E)$. Then the following norm equivalence is valid:*

$$\begin{aligned}&C_1\big(h_E\big\|\boldsymbol{\chi}^s(v_h)\big\|_{l^2}+\big\|\Pi_{k,E}^sv_h\big\|_{0,E}\big)\\&\le\|v_h\|_{0,E}\le C_2\big(h_E\big\|\boldsymbol{\chi}^s(v_h)\big\|_{l^2}+\big\|\Pi_{k,E}^sv_h\big\|_{0,E}\big).\end{aligned}\tag{3.34}$$

Proof. Since $SV_h^k(E)$ is a subspace of $V_h^k(E)$, then the lower bound holds true. We now prove the upper bound. By (3.33), (3.10) and the property that $\|m\|_{0,E}\le Ch_E$ for each $m\in M_{k/\beta_E}(E)$, we have

$$\begin{aligned}&\|v_h\|_{0,E}\le Ch_E\|\boldsymbol{\chi}(v_h)\|_{l^2}\\&\le Ch_E\big(\big\|\boldsymbol{\chi}^s(v_h)\big\|_{l^2}+|E|^{-1}|(v_h,m)_E|\big)\\&=Ch_E\big(\big\|\boldsymbol{\chi}^s(v_h)\big\|_{l^2}+|E|^{-1}\big|\big(\Pi_{k,E}^sv_h,m\big)_E\big|\big)\\&\le C\big(h_E\big\|\boldsymbol{\chi}^s(v_h)\big\|_{l^2}+\big\|\Pi_{k,E}^sv_h\big\|_{0,E}\big).\end{aligned}\tag{3.35}$$

Thus, we entails the bound (3.34). □

Remark 3.9. Based on Corollary 3.1, we can define the new computable stabilization terms on the serendipity virtual element space $SV_h^k(E)$

$$S_a^E(u_h,v_h):=\mathbf{A}_0^E\left(\sum_{i=1}^{N_{SD}}\chi_i^s(u_h)\chi_i^s(v_h)+|E|^{-1}\big(\Pi_{k,E}^su_h,\Pi_{k,E}^sv_h\big)_E\right),\tag{3.36}$$

$$S_b^E(u_h,v_h):=\rho_0^E|E|\left(\sum_{i=1}^{N_{SD}}\chi_i^s(u_h)\chi_i^s(v_h)+|E|^{-1}\big(\Pi_{k,E}^su_h,\Pi_{k,E}^sv_h\big)_E\right),\tag{3.37}$$

where $\mathbf{A}_0^E$ and ρ_0^E are the respective constant approximations of functions $\mathbf{A}$ and ρ on E.

Then we prove the following stability property.

Theorem 3.2. *The following stability bounds are valid:*

$$C_1 a^{\mathbf{A},E}(v_h,v_h) \le a_h^{\mathbf{A},E}(v_h,v_h) \le C_2 a^{\mathbf{A},E}(v_h,v_h), \quad \forall\, v_h \in SV_h^k(E), \quad \int_{\partial E} v_h \mathrm{d}s = 0, \tag{3.38}$$

$$C_1 b^E(v_h,v_h) \le b_h^E(v_h,v_h) \le C_2 b^E(v_h,v_h), \qquad \forall\, v_h \in SV_h^k(E). \tag{3.39}$$

Proof. It follows from the definition of the L^2-projection $\mathbf{\Pi}_{k-1,E}^0$ that the following orthogonality holds true:

$$\|\nabla v_h\|_{0,E}^2 = \big\|\mathbf{\Pi}_{k-1,E}^0 \nabla v_h\big\|_{0,E}^2 + \big\|\nabla v_h - \mathbf{\Pi}_{k-1,E}^0 \nabla v_h\big\|_{0,E}^2. \tag{3.40}$$

By (3.40), (3.2) and (3.34), we have

$$\begin{aligned}
&a^{\mathbf{A},E}(v_h,v_h) \le C\|\nabla v_h\|_{0,E}^2\\
&= C\Big(\big\|\mathbf{\Pi}_{k-1,E}^0 \nabla v_h\big\|_{0,E}^2 + \big\|\nabla v_h - \mathbf{\Pi}_{k-1,E}^0 \nabla v_h\big\|_{0,E}^2\Big)\\
&\le C\Big(\big\|\mathbf{\Pi}_{k-1,E}^0 \nabla v_h\big\|_{0,E}^2 + \|\nabla v_h\|_{0,E}^2\Big)\\
&\le C\Big(\big\|\mathbf{\Pi}_{k-1,E}^0 \nabla v_h\big\|_{0,E}^2 + h_E^{-2}\|v_h\|_{0,E}^2\Big)\\
&\le C\Big(\big\|\mathbf{\Pi}_{k-1,E}^0 \nabla v_h\big\|_{0,E}^2 + \big\|\boldsymbol{\chi}^s(v_h)\big\|_{l^2}^2 + h_E^{-2}\big\|\Pi_{k,E}^s v_h\big\|_{0,E}^2\Big)\\
&\le C a_h^{\mathbf{A},E}(v_h,v_h),
\end{aligned} \tag{3.41}$$

which entails the lower bound in (3.38). On the other hand, by (3.29), (3.36), (3.34) and the Poincaré inequality, we have

$$\begin{aligned}
a_h^{\mathbf{A},E}(v_h,v_h) &\le C\Big(\big\|\mathbf{\Pi}_{k-1,E}^0 \nabla v_h\big\|_{0,E}^2 + \big\|\boldsymbol{\chi}^s(v_h)\big\|_{l^2}^2 + |E|^{-1}\big\|\Pi_{k,E}^s v_h\big\|_{0,E}^2\Big)\\
&\le C\big(\|\nabla v_h\|_{0,E}^2 + h_E^{-2}\|v_h\|_{0,E}^2\big) \le C a^{\mathbf{A},E}(v_h,v_h).
\end{aligned} \tag{3.42}$$

Thus, we complete the proof of (3.38). The proof of (3.39) is an immediate consequence of Corollary 3.1. □

We are in the position to define the serendipity virtual element scheme of (2.2): Find $(\lambda_h, u_h) \in \mathbb{R} \times SV_h^k$ with $\|u_h\|_0 = 1$ such that

$$\mathbb{A}_h(u_h,v_h) = \lambda_h b_h(u_h,v_h), \quad \forall\, v_h \in SV_h^k, \tag{3.43}$$

where

$$\begin{aligned}
\mathbb{A}_h(u_h,v_h) &:= \sum_{E\in\mathcal{T}_h} \big(a_h^{\mathbf{A},E}(u_h,v_h) + b_h^E(\rho u_h, v_h)\big),\\
b_h(u_h,v_h) &:= \sum_{E\in\mathcal{T}_h} b_h^E(u_h,v_h).
\end{aligned} \tag{3.44}$$

In order to consider the spectral approximation property, we need the following discrete source problem: Find $\mu_h \in SV_h^k$ such that

$$\mathbb{A}_h(\mu_h,v_h) = b_h(f_h,v_h), \quad \forall\, v_h \in SV_h^k, \tag{3.45}$$

where $f_h := \Pi_k^0 f$, which is the best approximation of f that allows the computability since $(f_h, v_h) = (f, \Pi_k^0 v_h)$.

Proposition 3.5. *The discrete source problem* (3.45) *is well-posed.*

Proof. The well-posedness of the problem (3.45) follows by combining the stability properties (3.38), (3.39) and the Lax-Milgram theorem. □

As the continuous case, we introduce the discrete solution operator

$$T_h : SV_h^k \ \rightarrow \ SV_h^k, \quad T_h f_h = \mu_h. \tag{3.46}$$

By the Riesz representation theorem again, the discrete solution operator T_h is well-defined and is also compact since its range is finite dimensional.

Note that the discrete solution operator T_h is well-defined only in SV_h^k, instead of the Sobolev space $H_0^1(\Omega)$, since the computation of the stabilization term $S_b^E(\cdot,\cdot)$ on the right-hand side needs the DoFs, which are defined only in SV_h^k. However, we have to analyze the convergence of T_h to T in the operator norm $\|\cdot\|_{\mathcal{L}(H_0^1(\Omega))}$ as h tends to zero, where the operator norm on $H_0^1(\Omega)$ is defined by

$$\|T\|_{\mathcal{L}(H_0^1(\Omega))} := \sup_{f\in H_0^1(\Omega)} \frac{\|Tf\|_1}{\|f\|_1}.$$

Then, inspired by [35, 53], we can define a project operator P_h from $H_0^1(\Omega)$ to SV_h^k by

$$(P_h u - u, v_h) = 0, \quad \forall\, u \in H_0^1(\Omega), \quad \forall\, v_h \in SV_h^k, \tag{3.47}$$

and we have the following estimate:

$$\|P_h u\|_0 \leq \|u\|_0, \quad \|P_h u - u\|_0 = \inf_{v_h \in SV_h^k} \|u - v_h\|_0. \tag{3.48}$$

Now we can define auxiliary solution operator $\widehat{T}_h := T_h P_h$ mapping from $H_0^1(\Omega)$ to SV_h^k, and its spectrum set $sp(\widehat{T}_h)$ and the corresponding eigenfunctions coincide with the counterparts of T_h.

4. Error Estimates

In this section, we prove the a priori and a posteriori error estimates, where most procedures are similar with the standard VEM and we just briefly sketch the proof.

4.1. The spectral approximation and a priori error estimates

Firstly, we consider the error bound between the corresponding source problems (2.4) and (3.45) to study the convergence of the serendipity VEM.

Theorem 4.1. *Let μ and μ_h be the solutions to the problems* (2.4) *and* (3.45)*, respectively. There exists a constant $C > 0$ such that*

$$\|\mu - \mu_h\|_1 \leq C h^{\min\{r,1\}} \|f\|_1. \tag{4.1}$$

Proof. Let $I_h\mu$ be the interpolation of μ on SV_h^k, which satisfies the error result in Theorem 3.1. By the triangular inequality, it follows that

$$\|\mu - \mu_h\|_1 \leq \|\mu - I_h\mu\|_1 + \|\mu_h - I_h\mu\|_1. \tag{4.2}$$

We estimate the second term on the right-hand side of (4.2) on the element level. Let $\mathbf{I}$ be the identity matrix. By the coercivity of $\mathbb{A}_h^E(\cdot\,,\cdot)$, (2.4), (3.45), Proposition 3.4, Theorem 3.2, Proposition 3.1, Theorem 3.1 and (2.5), we have

$$\begin{aligned}
&C\big\|\mu_h - I_h^E\mu\big\|_{1,E}^2 \le \mathbb{A}_h^E\big(\mu_h - I_h^E\mu, \mu_h - I_h^E\mu\big)\\
&\le \mathbb{A}_h^E\big(\mu_h, \mu_h - I_h^E\mu\big) - \mathbb{A}^E\big(\mu, \mu_h - I_h^E\mu\big) + a^{\mathbf{I},E}\big(\mu, \mu_h - I_h^E\mu\big)\\
&\quad - a_h^{\mathbf{I},E}\big(I_h^E\mu, \mu_h - I_h^E\mu\big) + b^E\big(\mu, \mu_h - I_h^E\mu\big) - b_h^E\big(I_h^E\mu, \mu_h - I_h^E\mu\big)\\
&= b\big(f_h - f, \mu_h - I_h^E\mu\big) + a^{\mathbf{I},E}\big(\mu - \mu_\pi, \mu_h - I_h^E\mu\big) + a_h^{\mathbf{I},E}\big(\mu_\pi - I_h^E\mu, \mu_h - I_h^E\mu\big)\\
&\quad + b^E\big(\mu - \mu_\pi, \mu_h - I_h^E\mu\big) + b_h^E\big(\mu_\pi - I_h^E\mu, \mu_h - I_h^E\mu\big)\\
&\le C\big(\|f - f_h\|_{0,E} + \|\mu - \mu_\pi\|_{1,E} + \big\|\mu - I_h^E\mu\big\|_{1,E}\big)\big\|\mu_h - I_h^E\mu\big\|_{1,E}\\
&\le C\big(h_E\|f\|_{1,E} + h_E^r\|\mu\|_{1+r,E}\big)\big\|\mu_h - I_h^E\mu\big\|_{1,E}\\
&\le Ch_E^{\min\{r,1\}}\|f\|_{1,E}\big\|\mu_h - I_h^E\mu\big\|_{1,E},
\end{aligned} \tag{4.3}$$

which implies that

$$\big\|\mu_h - I_h^E\mu\big\|_{1,E} \le Ch_E^{\min\{r,1\}}\|f\|_{1,E}. \tag{4.4}$$

Summing (4.4) over all elements and substituting into (4.2), we prove the estimate (4.1). □

To prove the spectral approximation, it is enough to prove the convergence of $\widehat{T}_h$ to the solution operator T in the operator norm $\|\cdot\|_{\mathcal{L}(H_0^1(\Omega))}$; see [5].

Theorem 4.2. *There exists a constant $C > 0$ such that*

$$\|T - \widehat{T}_h\|_{\mathcal{L}(H_0^1(\Omega))} \le Ch^{\min\{r,1\}}. \tag{4.5}$$

Proof. The proof of (4.5) can be obtained by the error estimate in Theorem 4.1 and the definitions of the solution operators T and $\widehat{T}_h$. □

Let λ be an eigenvalue of (2.2) with multiplicity m, and denote the corresponding eigenspace by $\mathcal{E}_\lambda$. Since $\widehat{T}_h \to T$ as h tends to zero, then there exist m discrete eigenvalues $\lambda_h^1, \ldots, \lambda_h^m$ that converge to λ and are repeated according to their respective multiplicities [5, Section 8]. We denote $\mathcal{E}_{\lambda_h}$ be the direct sum of the eigenspaces corresponding to the eigenvalues $\lambda_h^1, \ldots, \lambda_h^m$. For the subspaces X and Y of $H_0^1(\Omega)$, the gap $\hat{\delta}_{H_0^1(\Omega)}$ between X and Y is defined by

$$\hat{\delta}_{H_0^1(\Omega)}(X, Y) = \max\big\{\delta_{H_0^1(\Omega)}(X, Y), \delta_{H_0^1(\Omega)}(Y, X)\big\}, \tag{4.6}$$

where

$$\delta_{H_0^1(\Omega)}(X, Y) = \sup_{x\in X, \|x\|_1=1}\Big(\inf_{y\in Y}\|x - y\|_1\Big),$$

analogously for $\delta_{H_0^1(\Omega)}(Y, X)$.

Thanks to [5, Theorems 7.1 and 7.3], we get the following spectral approximation.

Theorem 4.3. *Let λ be an eigenvalue of* (2.2) *associated to the eigenfunction u, then there exists an eigenvalue λ_h of* (3.43) *associated to the eigenfunction u_h such that*

$$\hat{\delta}_{H_0^1(\Omega)}(\mathcal{E}_\lambda, \mathcal{E}_{\lambda_h}) \le Ch^{\min\{r,k\}}, \tag{4.7}$$

$$|\lambda - \lambda_h| \le Ch^{\min\{r,k\}}. \tag{4.8}$$

Proof. We consider $f := \lambda u \in \mathcal{E}_\lambda \subseteq H^{1+r}(\Omega)$, then it follows from the same arguments in Theorem 4.1 that the following error estimate of the eigenfunction is valid:

$$\|u - u_h\|_1 \leq Ch^{\min\{r,k\}}\|u\|_{1+r}, \tag{4.9}$$

which implies that

$$\|(T - \widehat{T}_h)|_{\mathcal{E}_\lambda}\|_{\mathcal{L}(H_0^1(\Omega))} \leq Ch^{\min\{r,k\}}. \tag{4.10}$$

From [5, Theorems 7.1 and 7.3], we have

$$\hat{\delta}_{H_0^1(\Omega)}(\mathcal{E}_\lambda, \mathcal{E}_{\lambda_h}) \leq C\|(T - \widehat{T}_h)|_{\mathcal{E}_\lambda}\|_{\mathcal{L}(H_0^1(\Omega))}, \tag{4.11}$$

$$|\lambda - \lambda_h| \leq C\|(T - \widehat{T}_h)|_{\mathcal{E}_\lambda}\|_{\mathcal{L}(H_0^1(\Omega))}. \tag{4.12}$$

Substituting (4.10) into (4.11) and (4.12), we entail (4.7) and (4.8). □

We can observe from the coarse error estimate (4.8) that the convergence rate $\mathcal{O}(h^{\min\{r,k\}})$ of the numerical eigenvalues is suboptimal. Next, we improve the error estimate for the serendipity VEM approximation of eigenvalues.

Theorem 4.4. *There exists a constant $C > 0$ such that*

$$|\lambda - \lambda_h| \leq Ch^{2\min\{r,k\}}. \tag{4.13}$$

Proof. From (2.2) and (3.43), we have

$$\begin{aligned}(\lambda_h - \lambda)b(u_h, u_h) = {} & \mathbb{A}(u - u_h, u - u_h) - \lambda b(u - u_h, u - u_h) \\ & + \mathbb{A}_h(u_h, u_h) - \mathbb{A}(u_h, u_h) + \lambda_h\big(b(u_h, u_h) - b_h(u_h, u_h)\big).\end{aligned} \tag{4.14}$$

We estimate all terms on the right-hand side on the element level. By (3.32), (3.12), (3.38), (3.39), (3.28), (4.9) and Proposition 3.1, we have

$$\begin{aligned}&\mathbb{A}^E(u - u_h, u - u_h) - \lambda b^E(u - u_h, u - u_h) + \mathbb{A}_h^E(u_h, u_h) \\ &\quad - \mathbb{A}^E(u_h, u_h) + \lambda_h\big(b^E(u_h, u_h) - b_h^E(u_h, u_h)\big) \\ &\leq C\big(\|u - u_h\|_{1,E}^2 + a_h^{\mathbf{I},E}(u_h, u_h) - a^{\mathbf{I},E}(u_h, u_h) + b_h^E(u_h, u_h) - b^E(u_h, u_h)\big) \\ &= C\Big(\|u - u_h\|_{1,E}^2 + a_h^{\mathbf{I},E}\big(u_h - \Pi_{k,E}^\nabla u_h, u_h - \Pi_{k,E}^\nabla u_h\big) + a^{\mathbf{I},E}\big(\Pi_{k,E}^\nabla u_h - u_h, u_h - \Pi_{k,E}^\nabla u_h\big) \\ &\qquad + b_h^E\big(u_h - \Pi_{k,E}^0 u_h, u_h - \Pi_{k,E}^0 u_h\big) + b^E\big(\Pi_{k,E}^0 u_h - u_h, u_h - \Pi_{k,E}^0 u_h\big)\Big) \\ &\leq C\Big(\|u - u_h\|_1^2 + \big|u_h - \Pi_{k,E}^\nabla u_h\big|_{1,E}^2 + \big\|u_h - \Pi_k^0 u_h\big\|_0^2\Big) \leq Ch^{2\min\{r,k\}}.\end{aligned}$$

Summing the above bound over all elements and recalling the assumption that $\|u_h\|_0 = 1$, we complete the proof. □

4.2. A posteriori error estimates

In this section, we restrict to consider 2D case and then define an a posteriori error estimator for the serendipity VEM, whose reliability and efficiency can be proved. Let $\mathcal{B}_h^0$ denote the set of all interior edges of $\mathcal{T}_h$ and $\mathcal{B}_h^b$ denote the set of all boundary edges. For each $e \in \mathcal{B}_h^0$ shared by the elements E_1 and E_2, we denote the unit outer normal vector by $\boldsymbol{\nu}_e$ oriented from E_1

to E_2 (i.e., $\boldsymbol{\nu}_e = \boldsymbol{\nu}_{E_1}$). Then the jump of the normal derivative on e of a smooth function v is defined by

$$\begin{aligned}[\mathbf{A}\nabla v\cdot\boldsymbol{\nu}_e] &:= \mathbf{A}|_{E_1}\nabla(v|_{E_1})\cdot\boldsymbol{\nu}_{E_1} + \mathbf{A}|_{E_2}\nabla(v|_{E_2})\cdot\boldsymbol{\nu}_{E_2}\\ &= \big(\mathbf{A}|_{E_1}\nabla(v|_{E_1}) - \mathbf{A}|_{E_2}\nabla(v|_{E_2})\big)\cdot\boldsymbol{\nu}_e.\end{aligned}$$

The following lemma gives the derivation of the residual equation, which is the starting of the a posteriori error estimates.

Lemma 4.1. *Let (λ, u) and (λ_h, u_h) be the solutions of (2.2) and its discrete formulation (3.43), respectively. For any $v \in H_0^1(\Omega)$, we have*

$$\begin{aligned}\mathbb{A}(u-u_h,v) = \lambda b(u,v) - \lambda_h b(u_h,v) &+ \sum_{e\in\mathcal{B}_h}\int_e J_e v\mathrm{d}s\\ &- \sum_{E\in\mathcal{T}_h}\Big(a^{\mathbf{A},E}(u_h - \Pi^{\nabla}_{k,E}u_h, v)\\ &\qquad - b^E(R_E,v) - b^E\big((\lambda_h-\rho)\big(u_h-\Pi^0_{k,E}u_h\big),v\big)\Big),\end{aligned} \tag{4.15}$$

where we denote

$$\begin{aligned}R_E &:= \nabla\cdot\big(\mathbf{A}\nabla\Pi^{\nabla}_{k,E}u_h\big) + (\lambda_h-\rho)\Pi^0_{k,E}u_h,\\ J_e &:= \frac{1}{2}\big[\mathbf{A}\nabla\Pi^{\nabla}_{k,E}u_h\cdot\boldsymbol{\nu}_e\big],\quad \forall\, e\in\mathcal{B}_h^0,\quad J_e = 0,\quad \forall\, e\in\mathcal{B}_h^b.\end{aligned}$$

Proof. By (2.2) and integrating by parts, we have

$$\begin{aligned}\mathbb{A}(u-u_h,v) &= \lambda b(u,v) - \mathbb{A}(u_h,v)\\ &= \lambda b(u,v) - \sum_{E\in\mathcal{T}_h}\Big(a^{\mathbf{A},E}\big(u_h-\Pi^{\nabla}_{k,E}u_h,v\big) + a^{\mathbf{A},E}\big(\Pi^{\nabla}_{k,E}u_h,v\big)\\ &\qquad + b^E\big(\rho\big(u_h-\Pi^0_{k,E}u_h\big),v\big) + b^E\big(\rho\Pi^0_{k,E}u_h,v\big)\Big)\\ &= \lambda b(u,v) - \sum_{E\in\mathcal{T}_h}\Big(a^{\mathbf{A},E}\big(u_h-\Pi^{\nabla}_{k,E}u_h,v\big) - b^E\big(\nabla\cdot\big(\mathbf{A}\nabla\Pi^{\nabla}_{k,E}u_h\big),v\big)\\ &\qquad + \int_{\partial E}\big(\mathbf{A}\nabla\Pi^{\nabla}_{k,E}u_h\big)\boldsymbol{\nu}_E v\mathrm{d}s\\ &\qquad + b^E\big(\rho\big(u_h-\Pi^0_{k,E}u_h\big),v\big) + b^E\big(\rho\Pi^0_{k,E}u_h,v\big)\Big)\\ &= \lambda b(u,v) - \lambda_h b(u_h,v)\\ &\quad - \sum_{E\in\mathcal{T}_h}\Big(a^{\mathbf{A},E}\big(u_h-\Pi^{\nabla}_{k,E}u_h,v\big) - b^E\big(\nabla\cdot\big(\mathbf{A}\nabla\Pi^{\nabla}_{k,E}u_h\big) + (\lambda_h-\rho)\Pi^0_{k,E}u_h,v\big)\\ &\qquad - b^E\big((\lambda_h-\rho)\big(u_h-\Pi^0_{k,E}u_h\big),v\big)\Big) + \sum_{e\in\mathcal{B}_h}\int_e J_e v\mathrm{d}s,\end{aligned}$$

which entails the proof of the error equation (4.15). □

For each $E\in\mathcal{T}_h$, we introduce the local error estimator

$$\eta_E^2 := \big(\vartheta_a^E\big)^2 + \big(\vartheta_b^E\big)^2 + h_E^2\|R_E\|_{0,E}^2 + \sum_{e\in\partial E} h_E\|J_e\|_{0,e}^2, \tag{4.16}$$

where

$$\big(\vartheta_a^E\big)^2 := a_h^E\big(u_h - \Pi_{k,E}^{\nabla} u_h, u_h - \Pi_{k,E}^{\nabla} u_h\big),$$
$$\big(\vartheta_b^E\big)^2 := b_h^E\big(u_h - \Pi_{k,E}^{0} u_h, u_h - \Pi_{k,E}^{0} u_h\big).$$

Then the global error estimator η is defined by

$$\eta^2 := \sum_{E\in\mathcal{T}_h} \eta_E^2. \tag{4.17}$$

4.2.1. Reliability of the error estimator

The aim of this subsection is to prove the reliability of the error estimator. We first prove the error bound for the eigenfunction u with respect to the L^2-norm by the Aubin-Nitsche technique. Let (λ, u) and (λ_h, u_h) be the eigenpairs of (2.2) and (3.43), respectively. We consider the following dual problem: Find $p \in H_0^1(\Omega)$ such that

$$\mathbb{A}(\varphi, p) = b(\varphi, u - u_h), \quad \forall\, \varphi \in H_0^1(\Omega). \tag{4.18}$$

By the regularity assumption (2.5), we have

$$\|p\|_{1+r} \le C\|u - u_h\|_0. \tag{4.19}$$

Lemma 4.2. *There exists a constant $C > 0$ such that*

$$\|u - u_h\|_0 \le Ch^r\big(\|u - u_h\|_1 + \big|u_h - \Pi_k^{\nabla} u_h\big|_1 + \big\|u_h - \Pi_k^0 u_h\big\|_0\big). \tag{4.20}$$

Proof. Let $\varphi = u - u_h$ in (4.18), and $I_h^E p$ be the interpolation of p on $SV_h^k(E)$ that satisfies Theorem 3.1. We estimate (4.20) on the element level. From (4.18), (2.2), (3.43), (3.32), the definitions of $\Pi_{k,E}^0$ and $\Pi_{k,E}^{\nabla}$, it follows that

$$\begin{aligned}
\|u - u_h\|_{0,E}^2 &= \mathbb{A}^E(u - u_h, p)\\
&= \mathbb{A}^E\big(u - u_h, p - I_h^E p\big) + \mathbb{A}^E\big(u - u_h, I_h^E p\big)\\
&= \mathbb{A}^E\big(u - u_h, p - I_h^E p\big) + \mathbb{A}_h^E\big(u_h, I_h^E p\big)\\
&\quad - \mathbb{A}^E\big(u_h, I_h^E p\big) + \lambda b^E\big(u, I_h^E p\big) - \lambda_h b_h^E\big(u_h, I_h^E p\big)\\
&\le C\Big(\mathbb{A}^E\big(u - u_h, p - I_h^E p\big) + a_h^{\mathbf{I},E}\big(u_h, I_h^E p\big) - a^{\mathbf{I},E}\big(u_h, I_h^E p\big) + b_h^E\big(u_h, I_h^E p\big)\\
&\qquad - b^E\big(u_h, I_h^E p\big) + \lambda b^E\big(u, I_h^E p\big) - \lambda_h b_h^E\big(u_h, I_h^E p\big)\Big)\\
&= C\Big(\mathbb{A}^E\big(u - u_h, p - I_h^E p\big) + a_h^{\mathbf{I},E}\big(u_h - \Pi_{k,E}^{\nabla} u_h, I_h^E p - \Pi_{k,E}^0 p\big)\\
&\qquad + a^{\mathbf{I},E}\big(u_h - \Pi_{k,E}^{\nabla} u_h, \Pi_{k,E}^0 p - I_h^E p\big) + b_h^E\big(u_h - \Pi_{k,E}^0 u_h, I_h^E p - \Pi_{k,E}^0 p\big)\\
&\qquad + b^E\big(u_h - \Pi_{k,E}^0 u_h, \Pi_{k,E}^0 p - I_h^E p\big) + (\lambda - \lambda_h) b^E\big(u, I_h^E p\big)\\
&\qquad + \lambda_h b^E\big(u - \Pi_{k,E}^0 u, I_h^E p - \Pi_{k,E}^0 p\big) + \lambda_h b^E\big(\Pi_{k,E}^0(u - u_h), I_h^E p\big)\\
&\qquad + \lambda_h b_h^E\big(\Pi_{k,E}^0 u_h - u_h, I_h^E p - \Pi_{k,E}^0 p\big)\Big).
\end{aligned}$$

We can also conclude the following bound by the proof of Theorem 4.4:

$$|\lambda - \lambda_h| \le C\Big(\|u - u_h\|_1^2 + \big|u_h - \Pi_k^{\nabla} u_h\big|_1^2 + \big\|u_h - \Pi_k^0 u_h\big\|_0^2\Big). \tag{4.21}$$

Then, by (3.18), (3.38), (3.39), (3.3), (4.21), (4.9) and (4.19), we obtain

$$\|u-u_h\|_{0,E}^2 \le Ch_E^r\Big(\|u-u_h\|_{1,E}+\big|u_h-\Pi_{k,E}^{\nabla}u_h\big|_{1,E}+\big\|u_h-\Pi_{k,E}^{0}u_h\big\|_{0,E}\Big)\|u-u_h\|_{0,E},$$

which implies that we complete the proof. □

Next, we consider the upper bounds of the errors of numerical eigenfunctions and eigenvalues.

Theorem 4.5. *There exists a constant $C>0$ such that*

$$\|u-u_h\|_1+\big|u-\Pi_k^{\nabla}u_h\big|_1+\big\|u-\Pi_k^0u_h\big\|_0 \le C\eta, \tag{4.22}$$

$$|\lambda-\lambda_h| \le C\eta^2. \tag{4.23}$$

Proof. We firstly present the proof of (4.22) and denote $e:=u-u_h$. Using the coercive condition of $\mathbb{A}(\cdot,\cdot)$, the residual equation (4.15), (2.2) and (3.43), we obtain

$$\begin{aligned}
&C\|u-u_h\|_1^2 \le \mathbb{A}(u-u_h,e)\\
&=\mathbb{A}(u-u_h,e-I_he)+\mathbb{A}(u,I_he)-\mathbb{A}_h(u_h,I_he)+\mathbb{A}_h(u_h,I_he)-\mathbb{A}(u_h,I_he)\\
&=\lambda b(u,e-I_he)-\lambda_h b(u_h,e-I_he)\\
&\quad-\sum_{E\in\mathcal{T}_h}\Big(a^{\mathbf{A},E}\big(u_h-\Pi_{k,E}^{\nabla}u_h,e-I_he\big)\\
&\qquad\qquad-b^E\big(\nabla\cdot\big(\mathbf{A}\nabla\Pi_{k,E}^{\nabla}u_h\big)+(\lambda_h-\rho)\Pi_{k,E}^0u_h,e-I_he\big)\\
&\qquad\qquad-b^E\big((\lambda_h-\rho)\big(u_h-\Pi_{k,E}^0u_h\big),e-I_he\big)\Big)\\
&\quad+\lambda b(u,I_he)-\lambda_h b_h(u_h,I_he)+\mathbb{A}_h(u_h,I_he)-\mathbb{A}(u_h,I_he)+\sum_{e\in\mathcal{B}_h}\int_e J_e(e-I_he)\mathrm{d}s\\
&=\underbrace{\lambda b(u,e)-\lambda_h b(u_h,e)}_{I}+\underbrace{\mathbb{A}_h(u_h,I_he)-\mathbb{A}(u_h,I_he)+\lambda_h\big(b(u_h,I_he)-b_h(u_h,I_he)\big)}_{II}\\
&\quad+\underbrace{\sum_{E\in\mathcal{T}_h}\Big(b^E\big((\lambda_h-\rho)\big(u_h-\Pi_{k,E}^0u_h\big),e-I_h^Ee\big)-a^{\mathbf{A},E}\big(u_h-\Pi_{k,E}^{\nabla}u_h,e-I_h^Ee\big)\Big)}_{III}\\
&\quad+\underbrace{\sum_{E\in\mathcal{T}_h}b^E\big(\nabla\cdot\big(\mathbf{A}\nabla\Pi_{k,E}^{\nabla}u_h\big)+(\lambda_h-\rho)\Pi_{k,E}^0u_h,e-I_h^Ee\big)+\sum_{e\in\mathcal{B}_h}\int_e J_e\big(e-I_h^Ee\big)\mathrm{d}s}_{IV}.
\end{aligned}\tag{4.24}$$

For the term I, we apply the assumption that $\|u\|_0=\|u_h\|_0=1$ and (4.20) to obtain

$$\begin{aligned}
I&=\lambda+\lambda_h-(\lambda+\lambda_h)b(u,u_h)=\lambda+\lambda_h-\frac{\lambda+\lambda_h}{2}\big(2-b(e,e)\big)\\
&=\frac{\lambda+\lambda_h}{2}b(e,e)\le Ch^r\Big(\|u-u_h\|_1+\big|u_h-\Pi_k^{\nabla}u_h\big|_1+\big\|u_h-\Pi_k^0u_h\big\|_0\Big)\|e\|_0.
\end{aligned}$$

By (3.32), (3.38), (3.39) and the Cauchy-Schwarz inequality, we get

$$\begin{aligned}
II&\le C\sum_{E\in\mathcal{T}_h}\Big(\big|a_h^{\mathbf{I},E}\big(u_h,I_h^Ee\big)-a^{\mathbf{I},E}\big(u_h,I_h^Ee\big)\big|+\big|b_h^E\big(u_h,I_h^Ee\big)-b^E\big(u_h,I_h^Ee\big)\big|\Big)\\
&\le C\sum_{E\in\mathcal{T}_h}\Big(\big|a_h^{\mathbf{I},E}\big(u_h-\Pi_{k,E}^{\nabla}u_h,I_h^Ee\big)+a^{\mathbf{I},E}\big(\Pi_{k,E}^{\nabla}u_h-u_h,I_h^Ee\big)\big|
\end{aligned}$$

$$
\begin{aligned}
&\quad + \big|b_h^E\big(u_h - \Pi_{k,E}^0 u_h, I_h^E e\big) + b^E\big(\Pi_{k,E}^0 u_h - u_h, I_h^E e\big)\big|\Big) \\
&\le C \sum_{E\in\mathcal{T}_h} \Big(a^{\mathbf{I},E}\big(u_h - \Pi_{k,E}^\nabla u_h, u_h - \Pi_{k,E}^\nabla u_h\big)^{\frac{1}{2}} + b^E\big(u_h - \Pi_{k,E}^0 u_h, u_h - \Pi_{k,E}^0 u_h\big)^{\frac{1}{2}}\Big)\|e\|_1 \\
&\le C \sum_{E\in\mathcal{T}_h} \big(\vartheta_a^E + \vartheta_b^E\big)\|e\|_1.
\end{aligned}
$$

As for the term III, similar arguments give

$$
III \le C \sum_{E\in\mathcal{T}_h} \big(\vartheta_a^E + \vartheta_b^E\big)\|e\|_1.
$$

By the Cauchy-Schwarz inequality, (3.18) and the local trace theorem [17, Lemma 14], we have

$$
\begin{aligned}
IV &\le C \sum_{E\in\mathcal{T}_h} \Big(\big\|\nabla\cdot\big(\mathbf{A}\nabla\Pi_{k,E}^\nabla u_h\big) + (\lambda_h - \rho)\Pi_{k,E}^0 u_h\big\|_{0,E}\big\|e - I_h^E e\big\|_{0,E} \\
&\qquad + \sum_{e\in\partial E} \|J_e\|_{0,e}\big\|e - I_h^E e\big\|_{0,e}\Big) \\
&\le C \sum_{E\in\mathcal{T}_h} \Big(h_E\big\|\nabla\cdot\big(\mathbf{A}\nabla\Pi_{k,E}^\nabla u_h\big) + (\lambda_h - \rho)\Pi_{k,E}^0 u_h\big\|_{0,E}\|e\|_{1,E} \\
&\qquad + \sum_{e\in\partial E} \|J_e\|_{0,e}\Big(h_E^{-\frac{1}{2}}\big\|e - I_h^E e\big\|_{0,E} + h_E^{\frac{1}{2}}\big|e - I_h^E e\big|_{1,E}\Big)\Big) \\
&\le C \sum_{E\in\mathcal{T}_h} \Big(h_E\big\|\nabla\cdot\big(\mathbf{A}\nabla\Pi_{k,E}^\nabla u_h\big) + (\lambda_h - \rho)\Pi_{k,E}^0 u_h\big\|_{0,E} + \sum_{e\in\partial E} h_E^{\frac{1}{2}}\|J_e\|_{0,e}\Big)\|e\|_1 \\
&\le C\Big[\sum_{E\in\mathcal{T}_h} \Big(h_E^2\big\|\nabla\cdot\big(\mathbf{A}\nabla\Pi_{k,E}^\nabla u_h\big) + (\lambda_h - \rho)\Pi_{k,E}^0 u_h\big\|_{0,E}^2 + \sum_{e\in\partial E} h_E\|J_e\|_{0,e}^2\Big)\Big]^{\frac{1}{2}}\|e\|_1.
\end{aligned}
$$

Substituting the above estimates into (4.24), we estimate the first term $\|u - u_h\|_1$ in (4.22) by using η. Using the triangular inequality, (3.38), (3.39) and (4.24), we can also estimate the other terms on the left-hand side of (4.22). Furthermore, by (4.21) and (4.22), the bound (4.23) immediately follows. □

4.2.2. Efficiency of the error estimator

In this section, we show that the defined error estimator is efficient to mark the desired refined elements. To estimate the bound, we make use of the definitions of bubble functions. Under the mesh assumptions, each element $E \in \mathcal{T}_h$ admits a shape-regular sub-triangulation $\mathcal{T}_h^E$ obtained by joining each vertex of E with the center of the disk S_D. From [26, 55], for each $E \in \mathcal{T}_h$, an element bubble function $\psi_E \in H_0^1(E)$ is defined piecewise as the sum of the cubic bubble functions for each element in $\mathcal{T}_h^E$; for each $e \in \partial E$, an edge bubble function ψ_e is defined piecewise as a quadratic function, which equals to 1 at the barycenter of e and vanishes on the elements in $\mathcal{T}_h^E$ that do not contain e. The following results will be used in what follows.

Lemma 4.3. *For $E \in \mathcal{T}_h$ and $e \in \partial E$, let ψ_E and ψ_e be the interior and edge bubble functions, respectively. Then there exists $C > 0$ such that*

$$
C^{-1}\|q_k\|_{0,E}^2 \le \int_E \psi_E q_k^2 \,\mathrm{d}\boldsymbol{x} \le C\|q_k\|_{0,E}^2, \quad \forall\, q_k \in \mathbb{P}_k(E), \tag{4.25}
$$

$$C^{-1}\|q_k\|_{0,E} \le \|\psi_E q_k\|_{0,E} + h_E\|\nabla(\psi_E q_k)\|_{0,E} \le C\|q_k\|_{0,E}, \quad \forall\, q_k \in \mathbb{P}_k(E), \tag{4.26}$$

$$C^{-1}\|q_k\|_{0,e}^2 \le \int_e \psi_e q_k^2 \,\mathrm{d}s \le C\|q_k\|_{0,e}^2, \qquad \forall\, q_k \in \mathbb{P}_k(e). \tag{4.27}$$

Moreover, for any $q_k \in \mathbb{P}_k(e)$, there exists the constant extension $q_k \in \mathbb{P}_k(E)$ of q_k in the normal direction to e (denoted by the same symbol q_k) such that

$$h_E^{-\frac{1}{2}}\|\psi_e q_k\|_{0,E} + h_E^{\frac{1}{2}}\|\nabla(\psi_e q_k)\|_{0,E} \le C\|q_k\|_{0,e}. \tag{4.28}$$

Theorem 4.6. *There exists a constant $C > 0$ such that*

$$\eta^2 \le C\Big(\|u-u_h\|_1^2 + \big|u-\Pi_k^\nabla u_h\big|_1^2 + \big\|u-\Pi_k^0 u_h\big\|_0^2 + osc^2\Big), \tag{4.29}$$

where osc denotes the bound of the oscillation terms and is defined by the following higher order terms:

$$osc := \sum_{E\in\mathcal{T}_h} osc_E := \sum_{E\in\mathcal{T}_h}\left(h_E^{k+1}\big\|\nabla\Pi_{k,E}^\nabla u_h\big\|_{0,E} + h_E^{k+2}\big\|\Pi_{k,E}^0 u_h\big\|_{0,E}\right). \tag{4.30}$$

Proof. We consider the local bound for the a posteriori error estimator and estimate each term in (4.16). For the first and second terms, it follows from (3.38) and (3.39), that

$$\begin{aligned}\big(\vartheta_a^E\big)^2 + \big(\vartheta_b^E\big)^2 &\le C\left(a^{\mathbf{I},E}\big(u_h-\Pi_{k,E}^\nabla u_h, u_h-\Pi_{k,E}^\nabla u_h\big) + b^E\big(u_h-\Pi_{k,E}^0 u_h, u_h-\Pi_{k,E}^0 u_h\big)\right)\\ &\le C\left(\|u-u_h\|_{1,E}^2 + \big|u-\Pi_{k,E}^\nabla u_h\big|_{1,E}^2 + \big\|u-\Pi_{k,E}^0 u_h\big\|_{0,E}^2\right).\end{aligned} \tag{4.31}$$

For the third term, let $\overline{R}_E$ be the $L^2(E)$-orthogonal projection of R_E onto $\mathbb{P}_k(E)$. From (4.25), (4.15) with $v = \psi_E\overline{R}_E$, (4.26), (4.20), (4.22), (4.23) and (3.3), we have

$$\begin{aligned}h_E^2\|R_E\|_{0,E}^2 &\le h_E^2\big(\|\overline{R}_E\|_{0,E}^2 + \|R_E-\overline{R}_E\|_{0,E}^2\big)\\ &\le Ch_E^2\left(\int_E \psi_E\overline{R}_E^2 \mathrm{d}\boldsymbol{x} + \|R_E-\overline{R}_E\|_{0,E}^2\right)\\ &= Ch_E^2\left(\int_E R_E(\psi_E\overline{R}_E)\mathrm{d}\boldsymbol{x} + \int_E(\overline{R}_E-R_E)(\psi_E\overline{R}_E)\mathrm{d}\boldsymbol{x} + \|R_E-\overline{R}_E\|_{0,E}^2\right)\\ &= Ch_E^2\Big(\mathbb{A}^E(u-u_h,\psi_E\overline{R}_E) + a^{\mathbf{A},E}\big(u_h-\Pi_{k,E}^\nabla u_h,\psi_E\overline{R}_E\big)\\ &\qquad - b^E\big((\lambda_h-\rho)\big(u_h-\Pi_{k,E}^0 u_h\big),\psi_E\overline{R}_E\big)\\ &\qquad + \lambda_h b^E(u_h,\psi_E\overline{R}_E) - \lambda b^E(u,\psi_E\overline{R}_E)\\ &\qquad + b^E(\overline{R}_E-R_E,\psi_E\overline{R}_E) + \|R_E-\overline{R}_E\|_{0,E}^2\Big)\\ &\le Ch_E^2\Big(\|u-u_h\|_{1,E}\|\psi_E\overline{R}_E\|_{1,E} + \big|u-\Pi_{k,E}^\nabla u_h\big|_{1,E}|\psi_E\overline{R}_E|_{1,E}\\ &\qquad + \big\|u-\Pi_{k,E}^0 u_h\big\|_{0,E}\|\psi_E\overline{R}_E\|_{0,E} + (|\lambda_h-\lambda| + \|u_h-u\|_{0,E})\|\psi_E\overline{R}_E\|_{0,E}\\ &\qquad + \|\overline{R}_E-R_E\|_{0,E}\|\psi_E\overline{R}_E\|_{0,E} + \|R_E-\overline{R}_E\|_{0,E}^2\Big)\\ &\le Ch_E^2\Big(h_E^{-1}\big(\|u-u_h\|_{1,E} + \big|u-\Pi_{k,E}^\nabla u_h\big|_{1,E}\big) + \big\|u-\Pi_{k,E}^0 u_h\big\|_{0,E} + h_E^r\eta_E\\ &\qquad + \|R_E-\overline{R}_E\|_{0,E}\Big)\|R_E\|_{0,E},\end{aligned}$$

which implies that

$$\begin{aligned}h_E\|R_E\|_{0,E} \le C\Big(&\|u-u_h\|_{1,E} + \big|u-\Pi_{k,E}^\nabla u_h\big|_{1,E}\\ &+ h_E\big\|u-\Pi_{k,E}^0 u_h\big\|_{0,E} + h_E\|R_E-\overline{R}_E\|_{0,E} + h_E^{1+r}\eta_E\Big).\end{aligned} \tag{4.32}$$

For the fourth term, when $e \in \mathcal{B}_h^0$ shared by the elements E_1 and E_2 (one of them is E itself), let $\overline{J}_e$ be the $L^2(e)$-orthogonal projection of J_e onto $\mathbb{P}_k(e)$. By (4.27), (4.15) with $v = \psi_e\overline{J}_e$, (4.28), (4.20), (4.22), (4.23) and (3.3), it follows that

$$
\begin{aligned}
h_E\|J_e\|_{0,e}^2 &\le h_E\big(\|\overline{J}_e\|_{0,e}^2 + \|J_e - \overline{J}_e\|_{0,e}^2\big)\\
&\le h_E\left(\int_e \psi_e\overline{J}_e^2\mathrm{d}s + \|J_e - \overline{J}_e\|_{0,e}^2\right)\\
&= Ch_E\left(\int_e J_e(\psi_e\overline{J}_e)\mathrm{d}s + \int_e(\overline{J}_e - J_e)(\psi_e\overline{J}_e)\mathrm{d}s + \|J_e - \overline{J}_e\|_{0,e}^2\right)\\
&= Ch_E\Bigg(\mathbb{A}^E(u-u_h,\psi_e\overline{J}_e) + a^{\mathbf{A},E}\big(u_h - \Pi_{k,E}^{\nabla}u_h,\psi_e\overline{J}_e\big)\\
&\qquad - b^E(R_E,\psi_e\overline{J}_e) + \lambda_h b^E(u_h,\psi_e\overline{J}_e) - \lambda b^E(u,\psi_e\overline{J}_e)\\
&\qquad - b^E\big((\lambda_h-\rho)\big(u_h - \Pi_{k,E}^0u_h\big),\psi_e\overline{J}_e\big)\\
&\qquad + \int_e(\overline{J}_e - J_e)(\psi_e\overline{J}_e)\mathrm{d}s + \|J_e - \overline{J}_e\|_{0,e}^2\Bigg)\\
&\le Ch_E\Bigg(\|u-u_h\|_{1,E}\|\psi_e\overline{J}_e\|_{1,E} + \big|u - \Pi_{k,E}^{\nabla}u_h\big|_{1,E}|\psi_e\overline{J}_e|_{1,E}\\
&\qquad + \big\|u - \Pi_{k,E}^0u_h\big\|_{0,E}\|\psi_e\overline{J}_e\|_{0,E} + \|R_E\|_{0,E}\|\psi_e\overline{J}_e\|_{0,E}\\
&\qquad + (|\lambda-\lambda_h| + \|u-u_h\|_{0,E})\|\psi_e\overline{J}_e\|_{0,E}\\
&\qquad + \int_e(\overline{J}_e - J_e)(\psi_e\overline{J}_e)\mathrm{d}s + \|J_e - \overline{J}_e\|_{0,e}^2\Bigg),
\end{aligned}
$$

which implies by (4.32) that

$$
\begin{aligned}
h_E^{\frac12}\|J_e\|_{0,e} \le C\Big(&\|u-u_h\|_{1,E} + \big|u - \Pi_{k,E}^{\nabla}u_h\big|_{1,E} + h_E\big\|u - \Pi_{k,E}^0u_h\big\|_{0,E}\\
&+ h_E^{1+r}\eta_E + h_E\|R_E - \overline{R}_E\|_{0,E} + h_E^{\frac12}\|J_e - \overline{J}_e\|_{0,e}\Big).
\end{aligned}
\tag{4.33}
$$

To complete the proof, we need to provide a bound for the oscillation terms $h_E\|R_E-\overline{R}_E\|_{0,E}$ and $h_E^{1/2}\|J_e-\overline{J}_e\|_{0,e}$ in (4.32) and (4.33). We denote by $\mathbf{A}_h$ and ρ_h the piecewise polynomial approximations of the coefficients $\mathbf{A}$ and ρ, respectively. By the triangular inequality, the Cauchy-Schwarz inequality, the following polynomial trace inequality, see e.g., [22, Section 2.1.2]:

$$
\|p_k\|_{0,\partial E} \le Ch_E^{-\frac12}\|p_k\|_{0,E}, \quad \forall\, p_k \in \mathbb{P}_k(E),
$$

(3.3) and the property that $h_e \approx h_E$, we have

$$
\begin{aligned}
&h_E\|R_E - \overline{R}_E\|_{0,E} + h_E^{\frac12}\|J_e - \overline{J}_e\|_{0,e}\\
&\le h_E\Big(\big\|\nabla\cdot\big((\mathbf{A}-\mathbf{A}_h)\nabla\Pi_{k,E}^{\nabla}u_h\big)\big\|_{0,E} + \big\|\overline{\nabla\cdot\big((\mathbf{A}_h-\mathbf{A})\nabla\Pi_{k,E}^{\nabla}u_h\big)}\big\|_{0,E}\\
&\qquad + \big\|(\rho-\rho_h)\Pi_{k,E}^0u_h\big\|_{0,E} + \big\|\overline{(\rho_h-\rho)\Pi_{k,E}^0u_h}\big\|_{0,E}\Big)\\
&\qquad + h_E^{\frac12}\sum_{i=1,2}\Big(\big\|(\mathbf{A}-\mathbf{A}_h)|_{E_i}\nabla\big(\Pi_{k,E}^{\nabla}u_h|_{E_i}\big)\cdot\boldsymbol{\nu}_{E_i}\big\|_{0,e}\\
&\qquad\qquad + \big\|\overline{(\mathbf{A}_h-\mathbf{A})|_{E_i}\nabla\big(\Pi_{k,E}^{\nabla}u_h|_{E_i}\big)\cdot\boldsymbol{\nu}_{E_i}}\big\|_{0,e}\Big)\\
&\le h_E\Big(\|\nabla\cdot(\mathbf{A}-\mathbf{A}_h)\|_{0,E}\big\|\nabla\Pi_{k,E}^{\nabla}u_h\big\|_{0,E} + \|\rho-\rho_h\|_{0,E}\big\|\Pi_{k,E}^0u_h\big\|_{0,E}\Big)
\end{aligned}
$$

$$+ h_E^{\frac{1}{2}} \sum_{i=1,2} \Big(\|(\mathbf{A}_h - \mathbf{A})|_{E_i}\|_{0,e} \big\|\nabla \Pi_{k,E}^{\nabla} u_h|_{E_i}\big\|_{0,e} \Big)$$

$$\leq C\Big(h_E^{k+1} \big\|\nabla \Pi_{k,E}^{\nabla} u_h\big\|_{0,E} + h_E^{k+2} \big\|\Pi_{k,E}^{0} u_h\big\|_{0,E} \Big). \tag{4.34}$$

Inserting (4.31)-(4.34) into (4.16), we complete the proof. □

5. Numerical Results

In this section, we present the numerical examples to test the performance of the serendipity VEM and the effectiveness of the estimator. To escape from repetitive discussion, we present representative numerical results for the following a priori and a posteriori tests on different domains.

5.1. Square domain

In the first numerical test, we consider the Laplace eigenvalue problem (i.e., $\mathbf{A} = \mathbf{I}, \rho = 0$ in (2.1)) on the square domain $\Omega_S = [0,1]^2$, of which the initial meshes are shown in Fig. 5.1. The analytic solutions are known and the first four eigenvalues and associated eigenfunctions are

$$\begin{aligned}
\lambda_1 &= 2\pi^2 \approx 19.73920880218, \quad u_1(x,y) = \sin \pi x \sin \pi y,\\
\lambda_2 &= 5\pi^2 \approx 49.34802200545, \quad u_2(x,y) = \sin 2\pi x \sin \pi y,\\
\lambda_3 &= 5\pi^2 \approx 49.34802200545, \quad u_3(x,y) = \sin \pi x \sin 2\pi y,\\
\lambda_4 &= 8\pi^2 \approx 78.95683520872, \quad u_4(x,y) = \sin 2\pi x \sin 2\pi y.
\end{aligned}$$

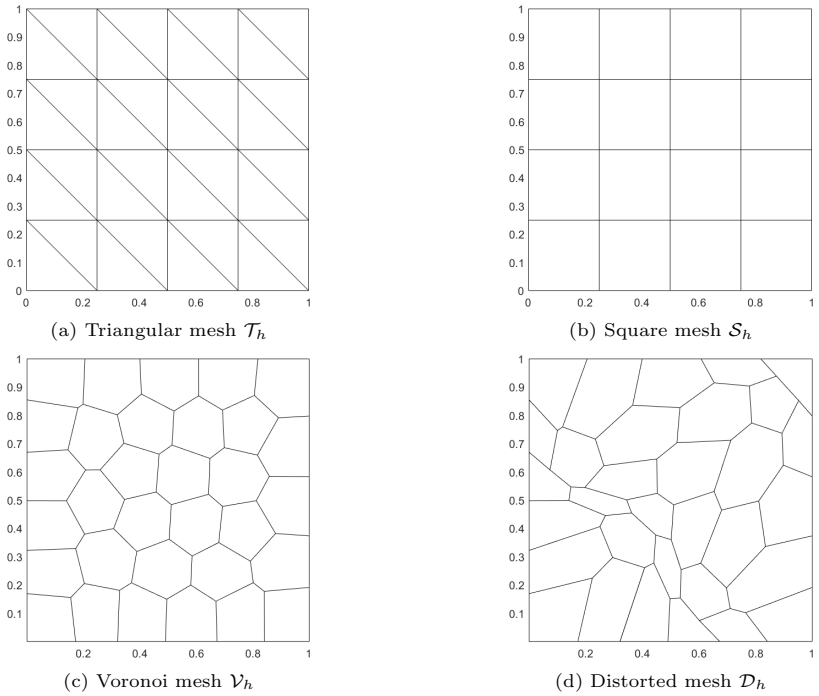

(a) Triangular mesh $\mathcal{T}_h$ (b) Square mesh $\mathcal{S}_h$

(c) Voronoi mesh $\mathcal{V}_h$ (d) Distorted mesh $\mathcal{D}_h$

Fig. 5.1. Illustration of initial meshes on Ω_S.

We observe that the regularity of the eigenfunctions is good enough, then by Theorem 4.4, the theoretical convergence rate of the approximate eigenvalue is $\mathcal{O}(N_S^{-k})$ as the number N_S of the DoFs increases, equivalently with theoretical result $\mathcal{O}(h^{2k})$.

We collect numerical results of the first four eigenvalues computed by the serendipity VEM on uniformly refined meshes in Tables 5.1 and 5.2 with the degrees of accuracy $k = 2, 3$, respectively. To observe the convergence rate, we apply error quantity Error $= |\lambda_{i,h} - \lambda_i|$, $i = 1, 2, 3, 4$ and also plot it in Figs. 5.2 and 5.3. It can be seen that these results are closer and closer to the exact result as the number of DoFs increases and attain the theoretical convergence order $\mathcal{O}(N_S^{-k})$. These phenomena are in agreement with Theorem 4.4.

To observe the reduction of the serendipity version, we list in Table 5.3 the number N of the DoFs for the standard VEM in [35]. Inspired by [10], we define the gain quantity as

$$\text{gain} := \frac{N - N_S}{N} \cdot 100\%,$$

Table 5.1: The first four eigenvalues computed by the serendipity VEM of uniformly refined meshes $\mathcal{T}_h$ and $\mathcal{V}_h$ on Ω_S with $k = 2$.

Mesh	N_S	$\lambda_{1,h}$	$\lambda_{2,h}$	$\lambda_{3,h}$	$\lambda_{4,h}$
	81	19.80511862864	49.88233126563	50.38350608895	82.14264041563
	289	19.74364568305	49.38795256991	49.42159511154	79.21851797423
$\mathcal{T}_h$	1089	19.73949196405	49.35064428256	49.35281837744	78.97456753869
	4225	19.73922659674	49.34818803711	49.34832521282	78.95796774106
	16641	19.73920991589	49.34803241683	49.34804101129	78.95690638609
	163	19.77250373848	49.73632728772	49.84138100371	81.07067060385
	323	19.74653839006	49.44869227073	49.45967134689	79.44958120061
$\mathcal{V}_h$	639	19.74131061665	49.38109715456	49.37552274465	79.09918310735
	1265	19.73972036963	49.35546506305	49.35576579422	78.99372403323
	2533	19.73936337183	49.35008963672	49.35030999559	78.96621629284

Table 5.2: The first four eigenvalues computed by the serendipity VEM of uniformly refined meshes $\mathcal{S}_h$ and $\mathcal{D}_h$ on Ω_S with $k = 3$.

Mesh	N_S	$\lambda_{1,h}$	$\lambda_{2,h}$	$\lambda_{3,h}$	$\lambda_{4,h}$
	105	19.74056172360	49.37712222091	49.37712222091	79.35038809492
	369	19.73922928607	49.34846896417	49.34846896417	78.96224689439
$\mathcal{S}_h$	1377	19.73920911980	49.34802896636	49.34802896636	78.95691714427
	5313	19.73920880713	49.34802211413	49.34802211413	78.95683647920
	20865	19.73920880225	49.34802200714	49.34802200714	78.95683522852
	260	19.74086770122	49.38542746513	49.40083460631	79.33624219812
	516	19.73939751495	49.35476113850	49.35396625887	78.99829928865
$\mathcal{D}_h$	1022	19.73927180680	49.34941169365	49.35018374306	78.96738147127
	2025	19.73921758324	49.34828753145	49.34823426365	78.95816542498
	4055	19.73921005613	49.34804784297	49.34806306085	78.95702088083

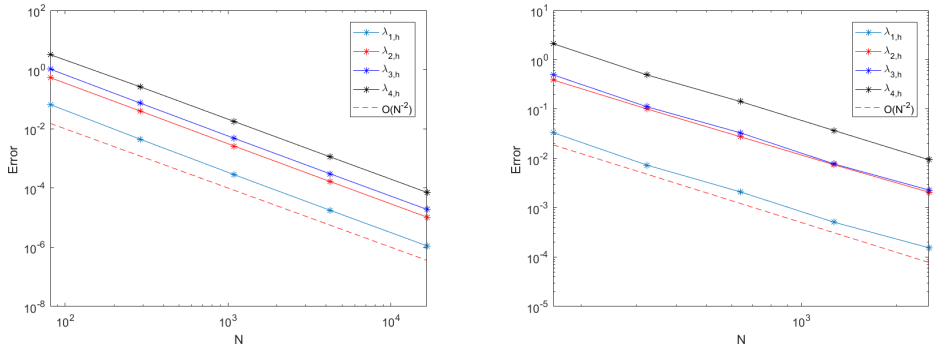

(a) $\mathcal{T}_h$ (b) $\mathcal{V}_h$

Fig. 5.2. The decay of error quantity with $k = 2$.

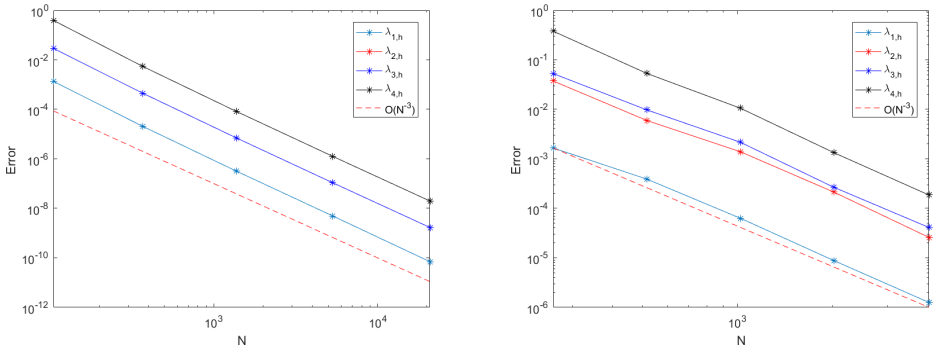

(a) $\mathcal{S}_h$ (b) $\mathcal{D}_h$

Fig. 5.3. The decay of error quantity with $k = 3$.

Table 5.3: The number of degrees of freedom for standard VEM on uniformly refined meshes and gain quantity.

Degree	Mesh	N (gain)				
$k = 2$	$\mathcal{T}_h$	113 (28.32%)	417 (30.70%)	1601 (31.98%)	6273 (32.65%)	24833 (32.99%)
	$\mathcal{V}_h$	195 (16.41%)	387 (16.54%)	767 (16.69%)	1521 (16.83%)	3045 (16.82%)
$k = 3$	$\mathcal{S}_h$	153 (31.37%)	561 (34.23%)	2145 (35.80%)	8385 (36.64%)	33153 (37.06%)
	$\mathcal{D}_h$	356 (26.97%)	708 (27.12%)	1406 (27.31%)	2793 (27.50%)	5591 (27.47%)

and show it in Table 5.3. Then obvious reduction of the DoFs for the serendipity VEM is observed. We underline that the gain quantity behaves differently and depends on the polygon shape. There exists a very slow increasing gain quantity in terms of refiner meshes, since more internal DoFs are allowed to be reduced.

Finally, Fig. 5.4 shows the eigenfunctions related to the first four Laplace eigenvalues.

5.2. Cube domain

In the second test, we consider the three-dimensional domain Ω_C and apply the polyhedral meshes $\mathcal{T}_h^1$, $\mathcal{T}_h^2$ and $\mathcal{T}_h^3$, where these polyhedral discretizations are made by translating the

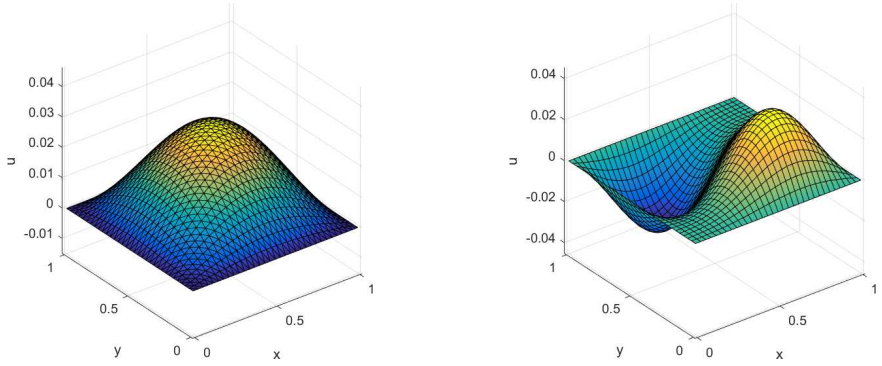

(a) $u_{1,h}$ (b) $u_{2,h}$

(c) $u_{3,h}$ (d) $u_{4,h}$

Fig. 5.4. The eigenfunctions related to the first four Laplace eigenvalues on Ω_S.

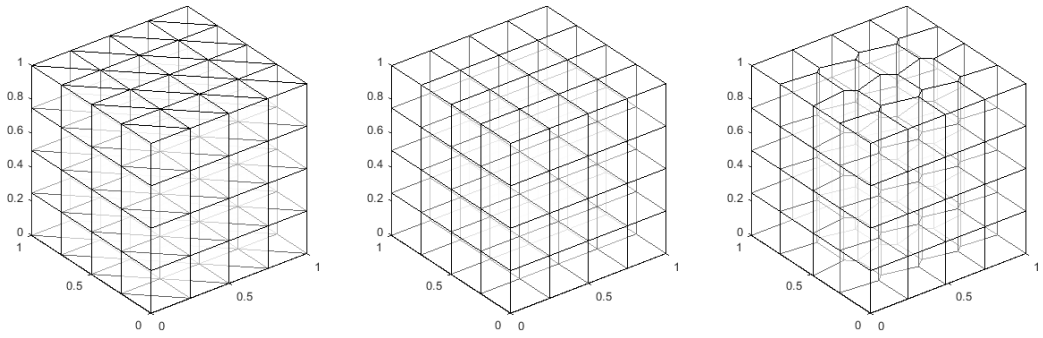

(a) $\mathcal{T}_h^1$ (b) $\mathcal{T}_h^2$ (c) $\mathcal{T}_h^3$

Fig. 5.5. Three families of polyhedral meshes on Ω_C.

two-dimensional polygonal meshes along the z-axis and connecting the corresponding vertices, as shown in Fig. 5.5.

The first four reference eigenvalues are computed by the FEM, where we compute the first four eigenvalues by using the finer tetrahedral mesh having 35937 nodes with the mesh size $h \approx 1.720\text{e-}02$ as follows:

$$\lambda_1 \approx 29.72777520806, \quad \lambda_2 \approx 59.57722486041,$$
$$\lambda_3 \approx 59.57722486041, \quad \lambda_4 \approx 59.78402168295.$$

In Tables 5.4 and 5.5, we present the obtained numerical results of the Laplace eigenvalues by the serendipity VEM using four families of polyhedral meshes on Ω_C, where we have applied the degree of accuracy $k = 1, 2$, respectively. Moreover, Figs. 5.6 and 5.7 depict the convergence curves and show that our algorithm achieves the optimal convergence rate $\mathcal{O}(N^{-2/3})$ for $k = 1$ and $\mathcal{O}(N^{-4/3})$ for $k = 2$. As shown in Table 5.6, the significant reduction of the DoFs for the 3D serendipity VEM is also observed for $k = 2$. We observe that the gain quantities are much bigger than those in Table 5.3, which implies that the serendipity technique is more meaningful in 3D case.

Table 5.4: The first four Laplace eigenvalues by using the sequences of meshes on Ω_C with $k = 1$.

Mesh	N_S	$\lambda_{1,h}$	$\lambda_{2,h}$	$\lambda_{3,h}$	$\lambda_{4,h}$
$\mathcal{T}_h^1$	125	47.04522167167	105.1941958954	129.1762864687	135.3734855988
	729	33.66266161653	69.42540373535	74.13850492131	75.05451093783
	4913	30.60788338250	61.71319310274	62.80274432682	63.03974102020
	35937	29.85780760858	59.83870638819	60.10548520736	60.16685069468
	274625	29.67101590714	59.37273500099	59.43907754746	59.45459349258
$\mathcal{T}_h^2$	125	45.78517343822	120.9424468173	120.9424468173	120.9424468173
	729	33.28942921915	71.84333212276	71.84333212276	71.84333212276
	4913	30.50878981309	62.22925654954	62.22925654954	62.22925654954
	35937	29.83258186898	59.96190213412	59.96190213412	59.96190213412
	274625	29.66467931862	59.40316215485	59.40316215485	59.40316215485
$\mathcal{T}_h^3$	170	46.80015363672	116.0458050673	124.1485217046	126.3686554167
	1098	33.34253304959	71.27547534211	72.03279496811	72.78817688763
	8857	30.42035480745	61.83935422286	61.87615027227	62.27808375195
	67650	29.81280664369	59.87312549179	59.88455184507	59.98999824570
	509535	29.66080242923	59.38600404197	59.38656573449	59.41415258316

Table 5.5: The first four Laplace eigenvalues by using the sequences of meshes on Ω_C with $k = 2$.

Mesh	N_S	$\lambda_{1,h}$	$\lambda_{2,h}$	$\lambda_{3,h}$	$\lambda_{4,h}$
$\mathcal{T}_h^1$	633	30.49302661733	62.56915987660	63.71269409718	64.86188084295
	4273	29.68230417798	59.50663977132	59.62407952327	59.70289629367
	52833	29.61394299317	59.23826813005	59.24808743845	59.25265918369
	239809	29.60914444424	59.21897026397	59.21965664493	59.21991627036
$\mathcal{T}_h^2$	489	30.78442033995	65.03993393114	65.03993393114	65.03993393114
	3185	29.69866847309	59.67856123530	59.67856123530	59.67856123530
	22881	29.61496563859	59.25043590982	59.25043590982	59.25043590982
	173249	29.60920836703	59.21976815972	59.21976815972	59.21976815972
$\mathcal{T}_h^3$	615	30.89106085098	64.97775318617	65.58394033103	66.34731963050
	4183	29.69373183102	59.67557925067	59.69527909037	59.70753292480
	34613	29.61332202947	59.24293789415	59.24335053746	59.24848276383
	267427	29.60910412011	59.21925976838	59.21929885061	59.21967878589

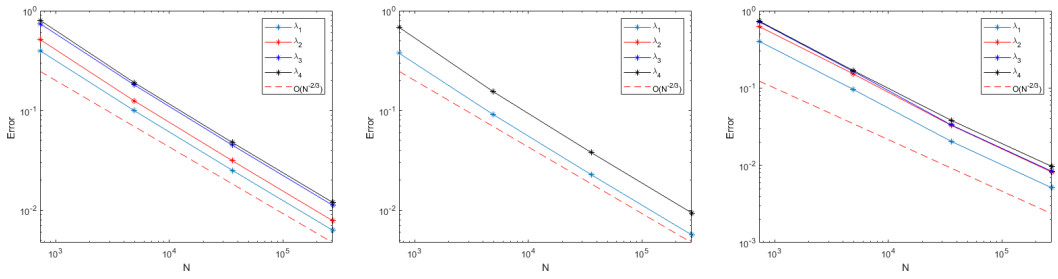

(a) $\mathcal{T}_h^1$ (b) $\mathcal{T}_h^2$ (c) $\mathcal{T}_h^3$

Fig. 5.6. The decay of error quantity with on D_C with $k = 1$.

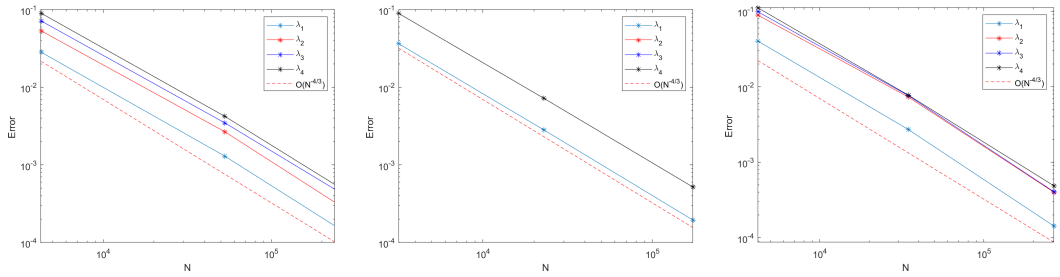

(a) $\mathcal{T}_h^1$ (b) $\mathcal{T}_h^2$ (c) $\mathcal{T}_h^3$

Fig. 5.7. The decay of error quantity with on D_C with $k = 2$.

Table 5.6: The number of degrees of freedom for standard VEM on uniformly refined meshes and gain quantity with $k = 2$ in 3D.

Mesh	N (gain)			
$\mathcal{T}_h^1$	1017 (60.66%)	7089 (65.90%)	31329 (68.64%)	407745 (70.03%)
$\mathcal{T}_h^2$	729 (49.08%)	4193 (54.25%)	35937 (57.06%)	274625 (58.52%)
$\mathcal{T}_h^3$	891 (44.88%)	6171 (47.53%)	51513 (48.83%)	399555 (49.41%)

5.3. L-shaped domain

The third test is used to test the performance of the estimator (4.17) for the Laplace eigenvalue problem on the L-shaped domain $\Omega_L = [-1, 1]^2 \setminus ((0, 1] \times (0, 1]))$. We fix the degree $k = 2$, apply the meshes $\mathcal{T}_h$ and $\mathcal{V}_h$, and only focus on the first eigenvalue. The sample meshes are plotted in Figs. 5.8(a) and 5.8(e). We obtain from [19] that the first eigenvalue on this domain is exactly approximated by $\lambda_1 \approx 9.6397238440219$ and its convergence order is lower than $\mathcal{O}(N_S^{-1})$, since the regularity index r in Theorem 4.4 of the eigenfunction related to the first eigenvalue is lower than one on the non-convex domain.

In Table 5.7, we display the numerical results of the serendipity VEM. The error of the first eigenvalue converges at the order of lower than $\mathcal{O}(N_S^{-1})$ even though we apply the serendipity VEM of the degree of accuracy $k = 2$.

In order to recover the optimal numerical performance of the first eigenvalue on the non-convex domain, we shall apply the adaptive virtual element algorithm based on the following loop:

(1) Set $it = 0$ and pick any initial mesh $\mathcal{T}_{it}$.

(2) Solve the eigenvalue problem (3.43) on $\mathcal{T}_{it}$.

(3) Estimate the local indicator η_E in (4.16).

(4) Mark elements to be subdivided according to the marking strategy that we choose to refine those elements in a set $\mathcal{M}_h \subseteq \mathcal{T}_h$ with minimum number such that

$$\sum_{E' \in \mathcal{M}_h} \eta_{E'}^2 \geq \gamma \sum_{E \in \mathcal{T}_h} \eta_E^2,$$

where γ is the marking parameter and is set to be 0.3.

(5) Refine these elements by the refinement strategy in [26], namely, connecting its barycenter to each edge midpoint.

(6) Let $it = it + 1$ and go back to step (2) until the stopping criterion, where we set the topping criterion as the error quality $|\lambda_{h,1} - \lambda_1| \leq 10^{-4}$.

We report the numerical results for the serendipity VEM with the adaptive triangular and Voronoi meshes. In Fig. 5.8, there contains some adaptively refined meshes representatively. We need 21 loops for the triangular mesh and 20 loops for Voronoi mesh to reach the stopping criterion. We observe that more elements are created around the origin. This fact shows that

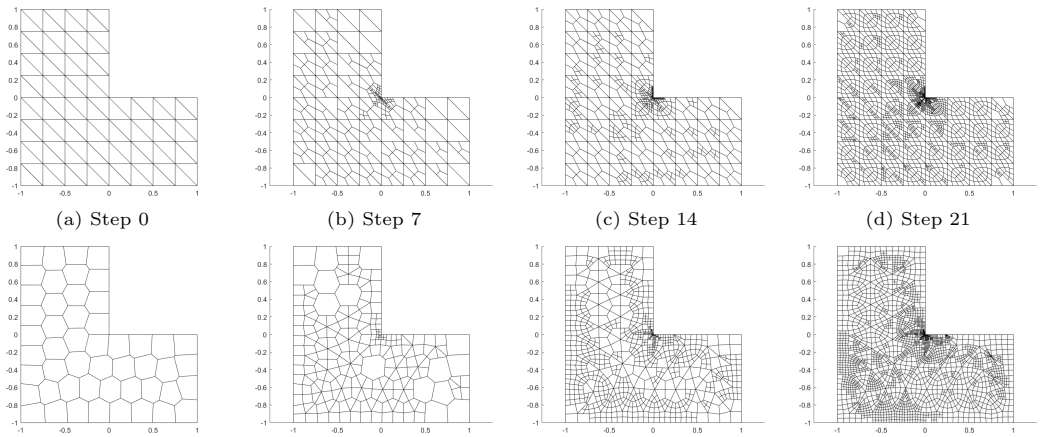

(a) Step 0 (b) Step 7 (c) Step 14 (d) Step 21

(e) Step 0 (f) Step 7 (g) Step 14 (h) Step 20

Fig. 5.8. Illustration of some adaptively refined triangular and Voronoi meshes.

Table 5.7: The first eigenvalue computed by the serendipity VEM of uniformly refined meshes $\mathcal{T}_h$ and $\mathcal{V}_h$ on Ω_L with $k = 2$.

$\mathcal{T}_h$				$\mathcal{V}_h$			
N_S	$\lambda_{1,h}$	Error	Rate	N_S	$\lambda_{1,h}$	Error	Rate
65	9.85582228	2.1610e-01	–	255	9.72999638	9.0273e-02	–
225	9.70299592	6.3272e-02	-0.98	503	9.69910051	5.9377e-02	-0.62
833	9.66360322	2.3879e-02	-0.75	1003	9.67671252	3.6989e-02	-0.69
3201	9.64915092	9.4271e-03	-0.69	3999	9.65843909	1.8715e-02	-0.49
12545	9.64346473	3.7409e-03	-0.68	7999	9.65260028	1.2876e-02	-0.54

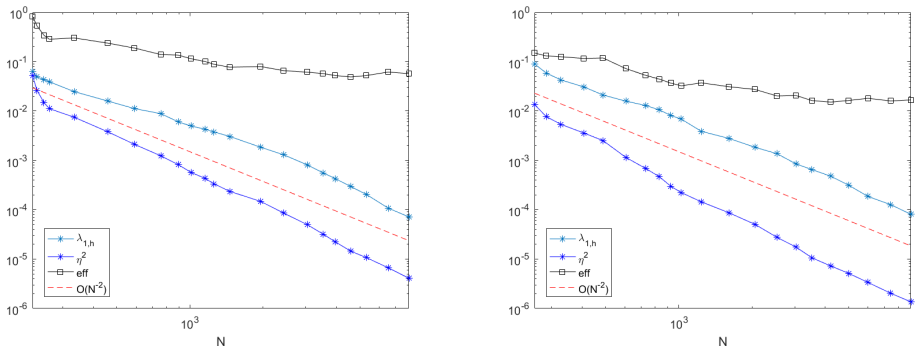

(a) $\mathcal{T}_h$ (b) $\mathcal{V}_h$

Fig. 5.9. The decay of error, estimator and effective index on adaptively refined triangular and Voronoi meshes.

the estimator can successfully capture the singularity at the reentrant corner. Then it can be seen from Fig. 5.9 that the adaptive scheme is able to recover the optimal convergence order $\mathcal{O}(N_S^{-2})$ of the approximate eigenvalue. Moreover, the error estimator converges with the same rate. Moreover, we compute the effective index

$$\text{eff} := \frac{\eta^2}{|\lambda_{h,1} - \lambda_1|},$$

which is close to a constant. The defined estimator used to drive the adaptive procedure shows to be reliable and efficient in the singularity case, which is in agreement with the theoretical results in Section 4.2.

5.4. The eigenvalue problems with small perturbed parameters

Finally, we are interested in the investigation of the singularly perturbed eigenvalue problems, where there is a the small enough perturbed parameter acting on the highest-order derivatives. Let $\mathbf{A} = \varepsilon^2\mathbf{I}$, where the parameter $0 < \varepsilon \ll 1$ is a non-negative real number and is usually known as a singularly perturbed parameter. Meanwhile, we take the coefficient function ρ as the harmonic potential $x^2 + y^2$. We now solve the self-adjoint second order elliptic eigenvalue problem (2.1) on $[-1, 1]^2$ by using the serendipity VEM with the degree $k = 1$ on uniform Voronoi meshes. In Table 5.8, we collect the numerical results of the first four eigenvalues with different perturbed parameters on $[-1, 1]^2$ decomposed by the finest Voronoi mesh. We see that the 1-st and 2-nd eigenvalues $\lambda_{i,h}$ have the following asymptotic behavior:

$$|\lambda_{i,h} - (2i)\varepsilon| \ \to \ 0, \quad \varepsilon \ \to \ 0^+,$$

Table 5.8: The first four eigenvalues of different perturbed parameters computed by the serendipity VEM with $k = 1$.

ε	$\lambda_{1,h}$	$\lambda_{2,h}$	$\lambda_{3,h}$	$\lambda_{4,h}$
0.1	0.20080339966	0.40272253028	0.40282169743	0.60559371301
0.05	0.10073910019	0.20213796978	0.20224757666	0.30452894895
0.025	0.05074354102	0.10214607559	0.10229145481	0.15441556224
0.00625	0.01332543817	0.02717592050	0.02741033433	0.04161667459

the 3-rd and 4-th eigenvalues $\lambda_{i,h}$ satisfy the following asymptotic behavior:

$$|\lambda_{i,h} - (2i-2)\varepsilon| \ \rightarrow \ 0, \quad \varepsilon \ \rightarrow \ 0^+.$$

From Fig. 5.10, the eigenfunctions shall be concentrated on the neighborhood of the origin point as $\varepsilon \rightarrow 0^+$. These phenomena are consistent with the theoretical analysis in [63]. Moreover, the numerical eigenvalues gradually become smaller with the same rate as the decreasing ε. However, the asymptotic analysis and uniform convergence of the VEM schemes for more general singularly perturbed eigenvalue problems are still open. We will study them in the future.

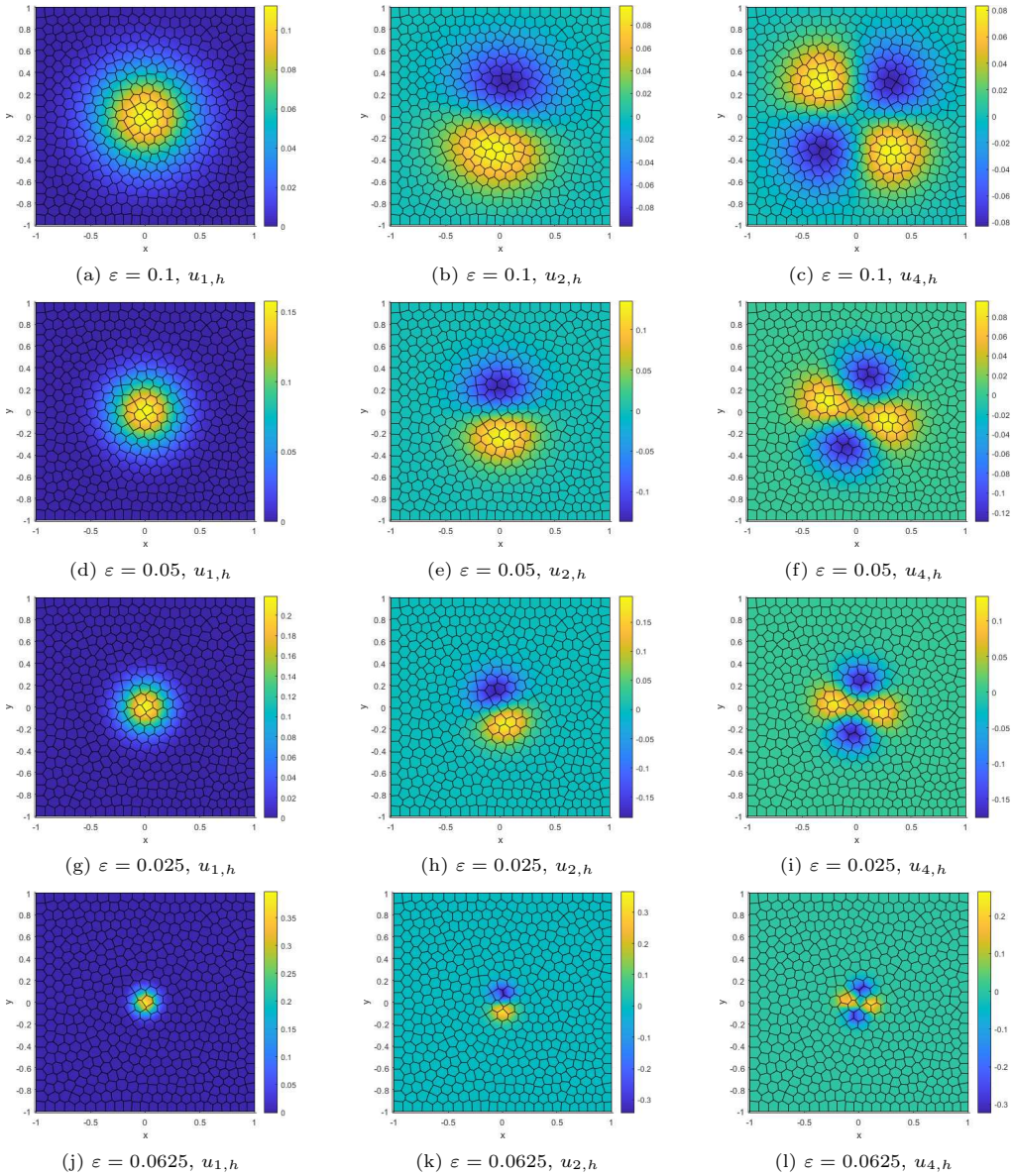

(a) $\varepsilon = 0.1$, $u_{1,h}$ (b) $\varepsilon = 0.1$, $u_{2,h}$ (c) $\varepsilon = 0.1$, $u_{4,h}$

(d) $\varepsilon = 0.05$, $u_{1,h}$ (e) $\varepsilon = 0.05$, $u_{2,h}$ (f) $\varepsilon = 0.05$, $u_{4,h}$

(g) $\varepsilon = 0.025$, $u_{1,h}$ (h) $\varepsilon = 0.025$, $u_{2,h}$ (i) $\varepsilon = 0.025$, $u_{4,h}$

(j) $\varepsilon = 0.0625$, $u_{1,h}$ (k) $\varepsilon = 0.0625$, $u_{2,h}$ (l) $\varepsilon = 0.0625$, $u_{4,h}$

Fig. 5.10. The eigenfunctions related to the singularly perturbed eigenvalues with different perturbed parameters.

6. Conclusion

In this paper, we have presented the a priori and a posteriori error estimates for the serendipity VEM of the self-adjoint second order elliptic eigenvalue problem theoretically and numerically. We has proved the optimal convergence rate and presented numerical results to demonstrate the theoretical results. On the other hand, we have constructed the residual-type a posteriori error estimator and proved reliable and efficient properties. Then we design an adaptive serendipity VEM algorithm. In order to complete the above theoretical analysis, we have also provided the interpolation theory and stability analysis for the given stabilization terms in the serendipity VEM scheme, which are fundamental tools in the analysis of serendipity virtual elements. The upcoming works shall investigate the more VEMs for the 2D and 3D singularly perturbed models.

Acknowledgements. The authors wish to thank the referees for constructive comments and suggestions.

This work is supported by the National Natural Science Foundation of China (Grant Nos. 12301532, 12371374, 12271523, 12071481, 12371198), and by the National University of Defense Technology (Grant Nos. 2023-lxy-fhjj-002, 202401-YJRC-XX-001).

References

[1] B. Ahmad, A. Alsaedi, F. Brezzi, L. Marini, and A. Russo, Equivalent projections for virtual element methods, *Comput. Math. Appl.*, **66**:3 (2013), 376–391.

[2] M. Ainsworth and T. Vejchodský, Robust error bounds for finite element approximation of reaction-diffusion problems with non-constant reaction coefficient in arbitrary space dimension, *Comput. Methods Appl. Mech. Engrg.*, **281** (2014), 184–199.

[3] P. Antonietti, A. Buffa, and I. Perugia, Discontinuous Galerkin approximation of the Laplace eigenproblem, *Comput. Methods Appl. Mech. Engrg.*, **195** (2006), 3483–3503.

[4] I. Babuška and J. Osborn, Finite element Galerkin approximation of the eigenvalues and eigenfunctions of selfadjoint problems, *Math. Comp.*, **52**:186 (1989), 275–297.

[5] I. Babuška and J. Osborn, Eigenvalue problems, in: *Handbook of Numerical Analysis*, Vol. II, North-Holland, (1991), 641–787.

[6] I. Babuška and W. Rheinboldt, Error estimates for adaptive finite element computations, *SIAM J. Numer. Anal.*, **15** (1978), 736–754.

[7] L. Beirão Da Veiga, F. Brezzi, A. Cangiani, G. Manzini, L. Marini, and A. Russo, Basic principles of virtual element methods, *Math. Models Methods Appl. Sci.*, **1** (2013), 199–214.

[8] L. Beirão Da Veiga, F. Brezzi, F. Dassi, L. Marini, and A. Russo, Virtual element approximation of 2D magnetostatic problems, *Comput. Methods Appl. Mech. Engrg.*, **327** (2017), 173–195.

[9] L. Beirão Da Veiga, F. Brezzi, F. Dassi, L. Marini, and A. Russo, A family of three-dimensional virtual elements with applications to magnetostatics, *SIAM J. Numer. Anal.*, **56**:5 (2018), 2940–2962.

[10] L. Beirão Da Veiga, F. Brezzi, F. Dassi, L. Marini, and A. Russo, Serendipity virtual elements for general elliptic equations in three dimensions, *Chinese Ann. Math. Ser. B*, **39**:2 (2018), 315–334.

[11] L. Beirão da Veiga, F. Brezzi, L. Marini, and A. Russo, Serendipity nodal VEM spaces, *Comput. Fluids*, **141**:15 (2016), 2–12.

[12] L. Beirão Da Veiga, F. Brezzi, L. Marini, and A. Russo, Virtual element methods for general second-order elliptic problems on polygonal meshes, *Math. Models Methods Appl. Sci.*, **26**:4 (2016), 729–750.

[13] L. Beirão Da Veiga, F. Brezzi, L. Marini, and A. Russo, Serendipity face and edge VEM spaces, *Rend. Lincei Mat. Appl.*, **28** (2017), 143–180.
[14] L. Beirão Da Veiga, F. Dassi, G. Manzini, and L. Mascotto, Virtual elements for Maxwell's equations, *Comput. Math. Appl.*, **116**:15 (2022), 82–99.
[15] L. Beirão Da Veiga and L. Mascotto, Stability and interpolation properties of serendipity nodal virtual elements, *Appl. Math. Lett.*, **142** (2023), 108639.
[16] L. Beirão Da Veiga, L. Mascotto, and J. Meng, Interpolation and stability estimates for edge and face virtual elements of general order, *Math. Models Methods Appl. Sci.*, **32**:8 (2022), 1493–1529.
[17] L. Beirão Da Veiga, D. Mora, G. Rivera, and R. Rodríguez, A virtual element method for the acoustic vibration problem, *Numer. Math.*, **136**:3 (2017), 725–763.
[18] A. Bermúdez, R. Durán, A. Muschietti, R. Rodríguez, and J. Solomin, Finite element vibration analysis of fluid-solid systems without spurious modes, *SIAM J. Numer. Anal.*, **32** (1995), 1280–1295.
[19] T. Betcke and L. Trefethen, Reviving the method of particular solutions, *SIAM Rev.*, **47**:3 (2005), 469–491.
[20] D. Boffi, Finite element approximation of eigenvalue problems, *Acta Numer.*, **19** (2010), 1–120.
[21] D. Boffi, F. Brezzi, and F. Fortin, *Mixed Finite Element Methods and Applications*, in: *Springer Series in Computational Mathematics*, Vol. 44, Springer, 2013.
[22] S. Brenner, Q. Guan, and L.-Y. Sung, Some estimates for virtual element methods, *Comput. Methods Appl. Math.*, **17**:4 (2017), 553–574.
[23] S. Brenner and R. Scott, *The Mathematical Theory of Finite Element Methods*, in: *Texts in Applied Mathematics*, Vol. 15, Springer-Verlag, 2008.
[24] F. Cakoni, D. Colton, S. Meng, and P. Monk, Stekloff eigenvalues in inverse scattering, *SIAM J. Math. Anal.*, **76**:4 (2016), 1737–1763.
[25] V. Calo, M. Cicuttin, Q. Deng, and A. Ern, Spectral approximation of elliptic operators by the hybrid high-order method, *Math. Comput.*, **88** (2019), 1559–1586.
[26] A. Cangiani, E. Georgoulis, T. Pryer, and O. Sutton, A posteriori error estimates for the virtual element method, *Numer. Math.*, **137** (2017), 857–893.
[27] A. Cangiani, G. Manzini, and O. Sutton, Conforming and nonconforming virtual element methods for elliptic problems, *IMA J. Numer. Anal.*, **37**:3 (2016), 1317–1354.
[28] C. Carstensen and J. Gedicke, An oscillation-free adaptive FEM for symmetric eigenvalue problems, *Numer. Math.*, **118**:3 (2011), 401–427.
[29] O. Čertík, F. Gardini, G. Manzini, L. Mascotto, and G. Vacca, The p- and hp-versions of the virtual element method for elliptic eigenvalue problems, *Comput. Math. Appl.*, **79**:7 (2020), 2035–2056.
[30] O. Čertík, F. Gardini, G. Manzini, and G. Vacca, The virtual element method for eigenvalue problems with potential terms on polytopic meshes, *Appl. Math.*, **63**:3 (2018), 333–365.
[31] L. Chen and J. Huang, Some error analysis on virtual element methods, *Calcolo*, **55** (2018), 5.
[32] R. Durán, C. Padra, and R. Rodríguez, A posteriori error estimates for the finite element approximation of eigenvalue problems, *Math. Models Methods Appl. Sci.*, **13**:8 (2003), 1219–1229.
[33] E. Garau, P. Morin, and C. Zuppa, Convergence of adaptive finite element methods for eigenvalue problems, *Math. Models Methods Appl. Sci.*, **19**:5 (2009), 721–747.
[34] F. Gardini, G. Manzini, and G. Vacca, The nonconforming virtual element method for eigenvalue problems, *ESAIM Math. Model. Numer. Anal.*, **53**:3 (2019), 749–774.
[35] F. Gardini and G. Vacca, Virtual element method for second order elliptic eigenvalue problems, *IMA J. Numer. Anal.*, **38**:4 (2017), 2026–2054.
[36] S. Giani and I. Graham, A convergent adaptive method for elliptic eigenvalue problem, *SIAM J. Numer. Anal.*, **47**:2 (2009), 1067–1091.
[37] P. Grisvard, *Singularities in Boundary Value Problems*, MASSON, Springer, 1992.
[38] J. Huang and Y. Yue, Some estimates for virtual element methods in three dimensions, *Comput.*

Meth. Appl. Mat., **23**:1 (2023), 177–187.
[39] F. Jochmann, An H^s-regularity result for the gradient of solutions to elliptic equations with mixed boundary conditions, *J. Math. Anal. Appl.*, **238** (1999), 429–450.
[40] J. Kuttler, Direct methods for computing eigenvalues of the finite difference Laplacian, *SIAM J. Numer. Anal.*, **11** (1974), 732–740.
[41] M. Larson, A posteriori and a priori error analysis for finite element approximations of self-adjoint elliptic eigenvalue problems, *SIAM J. Numer. Anal.*, **38** (2000), 608–625.
[42] F. Lepe, D. Mora, G. Rivera and I. Velásquez, A virtual element method for the Steklov eigenvalue problem allowing small edges, *J. Sci. Comput.*, **88** (2021), 44.
[43] F. Lepe and G. Rivera, A virtual element approximation for the pseudostress formulation of the Stokes eigenvalue problem, *Comput. Methods Appl. Mech. Engrg.*, **379** (2021), 113753.
[44] D. Mao, L. Shen, and A. Zhou, Adaptive finite element algorithms for eigenvalue problems based on local averaging type a posteriori error estimates, *Adv. Comput. Math.*, **25** (2006), 135–160.
[45] J. Meng and L. Mei, The matrix domain and the spectra of a generalized difference operator, *J. Math. Anal. Appl.*, **470** (2019), 1095–1107.
[46] J. Meng and L. Mei, A mixed virtual element method for the vibration problem of clamped Kirchhoff plate, *Adv. Comput. Math.*, **46** (2020), 68.
[47] J. Meng and L. Mei, Virtual element method for the Helmholtz transmission eigenvalue problem of anisotropic media, *Math. Models Methods Appl. Sci.*, **32**:8 (2022), 1589–1631.
[48] J. Meng, G. Wang, and L. Mei, A lowest-order virtual element method for the Helmholtz transmission eigenvalue problem, *Calcolo*, **58**:1 (2021), 2.
[49] J. Meng, Y. Zhang, and L. Mei, A virtual element method for the Laplacian eigenvalue problem in mixed form, *Appl. Numer. Math.*, **156** (2020), 1–13.
[50] B. Mercier, J. Osborn, J. Rappaz, and P. Raviart, Eigenvalue approximation by mixed and hybrid methods, *Math. Comput.*, **36** (1981), 427–453.
[51] P. Monk, *Finite Element Methods for Maxwell's Equations*, Clarendon Press, 2003.
[52] G. Monzón, A virtual element method for a biharmonic Steklov eigenvalue problem, *Adv. Pure Appl. Math.*, **10**:4 (2019), 325–337.
[53] D. Mora and G. Rivera, A priori and a posteriori error estimates for a virtual element spectral analysis for the elasticity equations, *IMA J. Numer. Anal.*, **40** (2020), 322–357.
[54] D. Mora, G. Rivera, and R. Rodríguez, A virtual element menthod for the Steklov eigenvalue problem, *Math. Models Methods Appl. Sci.*, **25**:8 (2015), 1421–1445.
[55] D. Mora, G. Rivera, and R. Rodríguez, A posteriori error estimates for a virtual element menthod for the Steklov eigenvalue problem, *Comput. Math. Appl.*, **74**:9 (2017), 2172–2190.
[56] D. Mora, G. Rivera, and I. Velásquez, A virtual element method for the vibration problem of Kirchhoff plates, *ESAIM Math. Model. Numer. Anal.*, **52** (2018), 1437–1456.
[57] D. Mora and I. Velásquez, A virtual element method for the transmission eigenvalue problem, *Math. Models Methods Appl. Sci.*, **28**:14 (2018), 2803–2831.
[58] D. Mora and I. Velásquez, Virtual element for the buckling problem of Kirchhoff-Love plates, *Comput. Methods Appl. Mech. Engrg.*, **360** (2020), 112687.
[59] R. Rannacher, Nonconforming finite element methods for eigenvalue problems in linear plate theory, *Numer. Anal.*, **33** (1979), 23–42.
[60] Y. Saad, J. Chelikowsky, and S. Shontz, Numerical methods for electronic structure calculations of materials, *SIAM Rev.*, **52**:1 (2010), 3–54.
[61] J. Sun and A. Zhou, *Finite Element Methods for Eigenvalue Problems*, CRC Press, 2016.
[62] G. Wang, J. Meng, Y. Wang, and L. Mei, A priori and a posteriori error estimates for a virtual element method for the non-self-adjoint Steklov eigenvalue problem, *IMA J. Numer. Anal.*, **32**:8 (2021), 1493–1529.
[63] K. Wang and Z. Huang, Asymptotic analysis and numerical method for singularly perturbed eigenvalue problems, *SIAM J. Sci. Comput.*, **40**:6 (2018), A3293–A3321.

[64] Y. Xu, Z. Zhou, and J. Zhao, Error analysis of serendipity virtual element methods for semilinear parabolic integro-differential equations, *J. Sci. Comput.*, **100** (2024), 55.

[65] Y. Xu, Z. Zhou, and J. Zhao, Error analysis of the second-order serendipity virtual element method for semilinear pseudo-parabolic equations on curved domains, *J. Comput. Math.*, **42** (2024), 1743–1776.

[66] Q. Zhai, H. Xie, R. Zhang, and Z. Zhang, Acceleration of weak Galerkin methods for the Laplacian eigenvalue problem, *J. Sci. Comput.*, **79** (2019), 914–934.